https://doi.org/10.5194/egusphere-2026-2466
Preprint. Discussion started: 20 May 2026

Estimating attainable soil organic carbon and farm-level limiting factors across Australia's grain-growing regions

Billal Hossen [1], Patrick Filippi [1], Dhahi Al-Shammari [1], Nikolas Hoskin [1], Senani Karunaratne [3] and Thomas F.A. Bishop[1,2]

[1] Precision Agriculture, Hydrology & Geoinformation Science Laboratory, Sydney Institute of Agriculture, School of Life and Environmental Sciences, The University of Sydney, Sydney, Eveleigh, NSW 2015, Australia

2 Sydney Informatics Hub; The University of Sydney; Newtown, NSW 2042

[3]CSIRO Agriculture and Food, Black Mountain, Australian Capital Territory, Australia

Correspondence to: Billal Hossen (billal.hossen@sydney.edu.au)

Abstract. Soil Organic Carbon (SOC) is a determining factor of soil health and agricultural crop productivity. The SOC level has generally declined since European settlement in Australia, primarily due to the clearing of native vegetation for agricultural purposes. To enhance soil health and crop yield, it is necessary to determine the attainable SOC potential and site-specific soil constraints that limit SOC build-up. To achieve this, we applied a Boundary Line Analysis (BLA) model to a dataset consisting of 1,782 soil sample sites, collected from 72 farms across the grain-growing regions of Australia. Laboratory measured soil properties including clay content, electrical conductivity (EC), cation exchange capacity (CEC), pH, exchangeable sodium percentage (ESP), and silt+clay from both the topsoil (0-30 cm) and subsoil (30-60 cm) were used as predictors in two separate BLA model to assess attainable SOC levels in the topsoil (0-30 cm), representing topsoil-driven and subsoil-driven constraints, respectively. Upper-envelope functions between SOC and each predictor variable were derived using a locally estimated scatterplot smoothing (LOESS) model in the BLA framework. A separate BLA was performed for different rainfall regions across Australia to reflect differences in attainable SOC. Digital soil maps for each soil property for a case study farm in the Wimmera, Victoria, were used to illustrate how the BLA can be used to identify limiting factors at the within-field level. Next, we applied the developed BLA models to that case study farm to determine the attainable SOC at the farm scale across six key soil properties. The results of the entire regional BLA model revealed that the attainable SOC in the topsoil varied from 0.98 % (mean minimum) to 1.39 % (mean maximum), in contrast to a mean actual (measured) SOC of 0.68 % (SD = 0.37; IQR = 0.45 - 0.82) across the region. This signifies a sequestration potential of 0.3 - 0.71 % in the uppermost soil layer, depending on rainfall zones and management practices. In addition, digital maps of the case study farm generated by applying BLA-derived models to spatial layers of soil predictors determine the attainable SOC, show its spatial pattern, and identify the most limiting factors across soil depths. The resulting map also illustrates the potential SOC gain after ameliorating the constraints. This BLA model is reproducible and can be readily applied across the 72 individual farms in Australia (if they have Digital Soil Maps) to quantify attainable SOC and identify site-specific soil constraints. Thus, providing a rapid and effective decision-support tool for farmers and farm managers to implement site-specific soil and agronomic management, thereby improving soil carbon levels.

Keywords: Maximum attainable SOC, soil carbon benchmarking, SOC sequestration, digital soil mapping, site-specific soil management.

https://doi.org/10.5194/egusphere-2026-2466
Preprint. Discussion started: 20 May 2026

1. Introduction

Soil organic carbon (SOC) is one of the key factors in determining the health, sustainability, and productivity of soil (Nabiollahi et al., 2018; Castaldi et al., 2019; Zeraatpisheh et al., 2020; Keshavarzi et al., 2020). It has a strong positive correlation with various soil characteristics, including cation exchange capacity and soil tilth (Bünemann et al., 2018), and boosts soil water holding capacity (Bünemann et al., 2018; Mirchooli et al., 2020). Furthermore, it enhances the stability of soil aggregates (Wagner et al., 2007; Ayoubi et al., 2012; Bünemann et al., 2018; Wang et al., 2019), improves the availability and cycling of nutrients (Wang et al., 2019), and stops soil loss and consequently reduces land vulnerability (Mirchooli et al., 2020; Kiani-Harchegani and Sadeghi, 2020). Increased soil carbon storage has attracted attention worldwide because of SOC's several advantages for improving soil health and mitigating climate change (Poeplau and Don, 2023; Prout et al., 2022). SOC loss is a common phenomenon in agriculture, particularly in intensive agricultural landscapes under certain management practices, although SOC dynamics rely on carbon inputs and losses from the system. According to Sanderman et al. (2017), the use of intensive land management techniques has led to a global loss of 133 Gt carbon, while the use of conservational agricultural techniques has raised the amount of carbon in the soil (Jonard et al., 2017; Minasny et al., 2011; Tipping et al., 2017). However, it is crucial for the land to maintain an appropriate level of SOC to improve and sustain crop yield. Ma et al. (2023) using a dataset of 3,662 controlled field trials with 66,593 treatments across a broad range of soils, climates and management practices, reported that crop yield is increased with the rise of SOC up to an optimum level, 31.2-32.4 g kg^{-1} for rice, 12.7-13.4 g kg^{-1} for wheat, and 43.2-43.9 g kg^{-1} for maize, beyond which no further yield increases are reported. Determining and establishing benchmarks for low, medium, and high levels of SOC storage is complex. These thresholds are highly varied and dependent on a number of site-specific factors such as soil texture, agricultural management practices (Drexler et al., 2022; Prout et al., 2022) and soil-forming factors including parent material, topography, climate, organisms, time, and human intervention (Jenny, 1994; Richter and Yaalon, 2012). For example, research by Churchman et al. (2020) and Soinne et al. (2023) has demonstrated that soil texture is a significant predictor of SOC values. In addition, a comprehensive understanding of the individual soil properties that constrain SOC accumulation, as well as the extent to which they limit SOC potential, is essential for planning efficient soil management practices that improve agricultural output and sustain soil health. This necessitates not only identifying limiting factors but also mapping their spatial variability across fields or areas. However, this can be challenging because SOC is affected by multiple soil characteristics that interact together, making it difficult to identify the most limiting factors, particularly in a spatial context.

Multiple traditional and modern data-driven approaches are employed to identify relationships between SOC and other soil properties. These models are developed, in some cases, to estimate the potential or attainable SOC stocks under given conditions (Karunaratne et al., 2024). However, because they are calibrated using measured datasets across heterogeneous landscapes, there is no guarantee that all ecosystems represented are functioning without constraints. Consequently, such models are better interpreted as quantifying attainable SOC stocks rather than true potential SOC (Karunaratne et al., 2024). A range of statistical methods has been used to determine the attainable SOC or SOC potentials. Hassink (1997) used the relationship between SOC and the fine particle-size fraction (silt+clay) and fitted a linear least squares regression model to determine the maximum carbon storage capacity. A similar method was also applied in a number of other studies (Chen et al., 2019; Chenu et al., 2019; Gregorich et al., 2009; Wiesmeier et al., 2014; Beare et al., 2014; Jien et al., 2025). Georgiou et al. (2022) calculated the maximal SOC storage capacity at 1044 locations worldwide using quantile regression, and Karunaratne et al. (2024) also employed 90th quantile regression across 475 sites in Australian soils. Some studies used the Boundary Line Analysis (BLA) model to estimate SOC in different landscapes (Feng et al., 2013; Beare et al., 2014; Fujisaki et al.,2018; Wenzel et al., 2022). Viscarra Rossel et al. (2024) used the Frontier line analysis to estimate the maximum mineral-associated organic carbon (MAOC) storage capacity at 5089 sites across Australia for the topsoil (0-30 cm), which is conceptually similar to BLA, as both methods identify the upper limit or maximum potential response of a dependent variable.

https://doi.org/10.5194/egusphere-2026-2466
Preprint. Discussion started: 20 May 2026

However, a regression-based model fitting through the scatter of points, e.g. Hassink (1997), determines the SOC for a given property, does not estimate the maximum upper limit and does not isolate the non-limiting observation. The quantile-regression, frontier line and BLA approaches used in previous studies typically used a single predictor variable to estimate the SOC upper limit, without explicitly distinguishing which soil factor constrains SOC at an individual location. Because these models are calibrated against diverse field datasets, they cannot ensure that observations at the upper boundary are free of other constraints. As a result, although they estimate the attainable SOC, they are unable to identify and map the limiting factor preventing locations from attaining that boundary. As will be described in detail later, a solution to this is the multivariate BLA framework as used by Shatar and McBratney (2004) to identify yield-limiting soil factors, which integrated several soil properties to estimate attainable crop yield while simultaneously identifying and spatially mapping the most limiting factors at each location across a single paddock.

BLA is a statistical technique that has been mainly used for determining the factors, typically soil properties, that limit crop yield. Webb (1972) was the first to introduce the BLA concept, which states that a biological reaction to a particular environmental variable is expressed only in a subset of observations in which other factors are not limiting. This method has been used to investigate numerous issues in agronomy, soil science, and biology (Milne et al., 2006a; Milne et al., 2006b). It has been employed to ascertain soil properties such as macro and micronutrients, SOC, and pH, which are linked to crop yield constraints (Huang et al., 2008; Patrignani et al., 2014; Shatar and McBratney, 2004; Tittonell and Giller, 2013). The approach seeks to determine the relationship between an input variable (x) and a response variable (y) with other variables not held constant or optimal (Makowski et al., 2007). This process involves fitting a line to the data cloud edge, which is often the upper part (Hajjarpoor et al., 2018). It is commonly used in agronomy where crop yield is the response variable, and a nutrient is the input variable. This "boundary line" indicates the maximum yield, also often referred to as yield potential, under a condition when a parameter of interest lies on the x-axis. Because of this, yields at the boundary line are thought to be the highest values in big datasets when limiting factors are absent, while all sites below the line are thought to be constrained by other factors not considered (e.g., soil texture, soil pH, or moisture content). The process of fitting a boundary line (BL) to the upper limit of agricultural data is not universally accepted. When this method was first implemented, the BLA curves were visually fitted (Webb, 1972). In later methods, BL have been manually determined using data cloud maximum values (Hajjarpoor et al., 2018; Lewandowski and Schmidt, 2006), or the environmental variable has been split into "buckets" or movable windows along the x-axis to determine the upper quantile or maximum of each bucket (Schmidt et al., 2000; Shatar and McBratney, 2004). Although they are not as commonly utilised, some researchers have also employed more sophisticated statistical techniques (e.g. likelihood-based and accounting for the data being censored) to determine boundary lines (Lark and Milne, 2016; Lark et al., 2020; Makowski et al., 2007; Milne et al., 2006a).

As stated, BLA has been widely utilised to determine the potential crop yield and yield-limiting factors. Crop yields are evaluated in relation to different soil properties such as organic matter, nutrient concentration and pH (Casanova et al., 1999; Kitchen et al., 2003; Shatar and McBratney, 2004; Tittonell et al., 2008). Crop yields are also assessed in some studies based on precipitation (Huang et al., 2008), growing season rainfall (Patrignani et al., 2014), soil properties and nutrients (i.e., macro and micronutrients, SOC, and pH) (Shatar and McBratney, 2004; Lark et al., 2020), plant density (Tittonell and Giller, 2013), while using the BLA model. Wang et al. (2015) evaluated 254 coffee farms in Uganda and identified adverse soil nutritional status (low phosphorus and potassium), poor plant density, and high pH as significant yield-limiting variables, responsible for 45%-52% of the yield gap of coffee by implementing the BLA approach.

In this study, we developed six individual BLA models for six key soil properties to estimate attainable SOC. Afterwards, a multivariate BLA model was developed by integrating multiple univariate BLAs, which offers a robust and comprehensive framework for determining the location-specific limiting factor affecting a response variable (SOC). This concept was

https://doi.org/10.5194/egusphere-2026-2466
Preprint. Discussion started: 20 May 2026

demonstrated by Shatar and McBratney (2004), where they identified site-specific causes of yield variation and yield potentials by applying the law of minimum in a multivariate BLA model. The grain production system in Australia is categorised into three principal regions (Northern, Southern, and Western), which are further segmented into 13 agroecological zones determined by climate, soil properties, and prevailing cropping systems (GRDC, 2024). Regional and agroecological disparities generate significant heterogeneity in soil organic carbon (SOC) dynamics and sequestration capability within dryland systems. In acknowledgement of this heterogeneity, the study employed the BLA framework on a dataset from 72 geographically diverse dryland grain growing farms throughout these regions to estimate attainable SOC levels. Through the evaluation of SOC relationships with key soil properties in both topsoil and subsoil layers, our objectives were to: (i) develop and implement BLA framework to determine the attainable SOC (topsoil) for each rainfall regions at the national scale, (ii) use the BLA to identify and illustrate spatially the most limiting soil factor across the case study farm, and (iii) assess how the alleviation of particular limiting factors, ESP or EC, for example, could lift the attainable SOC values of the case study farm. Furthermore, we aimed to assess whether the suggested BLA framework may function as a spatial diagnostic instrument for pinpointing soil limitation zones by creating composite limiting-factor maps for both topsoil and subsoil.

2. Materials and Methods

2.1 Study area and dataset

The focus of this work is on 0-30 cm soil organic carbon in terms of its attainable levels and the soil properties that limit achieving this. The study area comprises 72 farms from across the grain-growing regions of Australia (Figure 1). These farms represented the 14 subregions, which were created based on the Grains Research and Development Corporation (GRDC) agroecological zones and adapted from the Brock et al. (2014) zones, which integrated climatic, agronomic, and ecological factors. These farms were selected with the assistance of growers or local consultants, with the primary objective of identifying an area representative of grain-cropping soils within the local region. Farm sizes vary between 215 and 1975 ha, with an average of 970 ha per farm. At each farm, 25 sampling sites were randomly selected using a stratified random sampling technique. Soil cores were sampled and analysed at four depth intervals to a maximum depth of 1 m (0-15 cm, 15-30 cm, 30-60 cm, 60-100 cm). This was performed following a similar approach to Filippi et al. (2024) and Wang et al. (2024), and further details can be found there, including the stratified random sampling approach across the selected farms. The soil dataset, including clay content, electrical conductivity (EC), cation exchange capacity (CEC), exchangeable sodium percentage (ESP), pH, and silt+clay from these 72 farms, was used to develop the BLA model for estimating attainable SOC. Six digital soil maps (DSMs) of these key soil properties were also created for a case study farm (details described later). The developed BLA model was then employed on these DSMs of the case study farm to generate a limiting factor map. The case study farm is located in the Wimmera region of Victoria, Australia, and falls within the Wimmera VIC SA grain-growing region as defined by the GRDC, which is highlighted in the white point in Figure 1.

The advantage of this dataset is that all farms were sampled in the same way over a 26-month period (2023-2025), targeted to grain growing farms and the same commercial laboratory was used, meaning it is a consistent dataset as compared to legacy soil datasets with varying lab analysis methods and imprecise land use information.

https://doi.org/10.5194/egusphere-2026-2466
Preprint. Discussion started: 20 May 2026

170

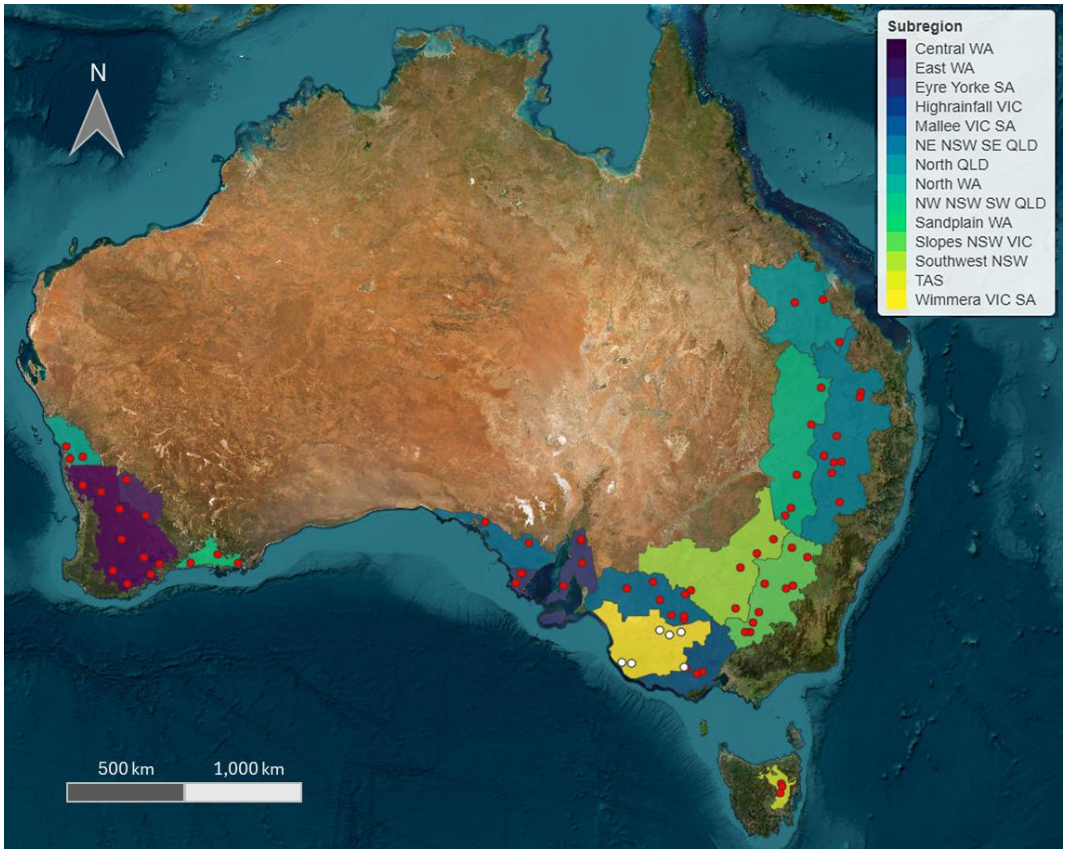

Figure 1: Location of farms sampled overlaying the grain-growing regions of Australia.

2.2 Allocation of the farm sites across the derived season rainfall classification

The study area encompasses diverse regions of Australia and encompasses a wide range of soil types, terrain, and climates. To facilitate significant regional-scale analysis of SOC constraints, the study area needed to be stratified into different regions. Although several classification frameworks exist, including the GRDC grain-growing regions, which have 14 subregions across Australia, we had 2-9 farms in each subregion, which we felt was not enough to perform a robust BLA for each. Instead, we decided on rainfall classification as rainfall has a significant impact on the potential of SOC accumulation and stabilisation (Minasny et al., 2013; Viscarra Rossel et al., 2014). Wetter regions typically offer larger SOC potential than drier ones, as rainfall regulates biomass production and organic matter input. Accordingly, datasets consisting of 72 farms were classified into six categories (Figure 2 and Table 1) based on the Australian Bureau of Meteorology's (BOM) seasonal rainfall zones (http://www.bom.gov.au/climate/maps/averages/climate-classification/?maptype=seasb) in order to capture this climatic influence. These regions classify places based on the time and distribution of annual precipitation, specifically summer-dominant, winter-dominant, uniform, and arid patterns and illustrate the varied climatic gradients that influence Australia's agroecosystems. Each farm was allocated to a rainfall region based on its geographic coordinates. Seasonal rainfall is a crucial factor influencing pedogenesis, nitrogen cycling, salinity dynamics, and organic carbon storage and overall farming productivity, with various regions displaying distinct climatic effects on soil processes and agricultural systems. For example, summer-dominant regions frequently experience intense rainfall and elevated temperatures that promote leaching and seasonal

https://doi.org/10.5194/egusphere-2026-2466
Preprint. Discussion started: 20 May 2026

nutrient variability, while also supporting summer cropping systems and higher biomass production when water availability coincides with plant growth. Conversely, winter-dominant regions, such as much of western Australia, experience most precipitation during the cooler months, thereby facilitating winter-based agricultural systems (e.g., cereals, canola, and pulses) and seasonal pastures, whereas limited summer rainfall restricts summer cropping or grazing. The BOM's seasonal rainfall classification was used in this study for pragmatic reasons; it gave 3-27 farms for each region, which was sufficient for BLA (Table 1). However, alternative classifications, such as the Koppen classification system or the GRDC subregions, could also be used to capture the climatic and environmental effects, especially if the datasets grow in size.

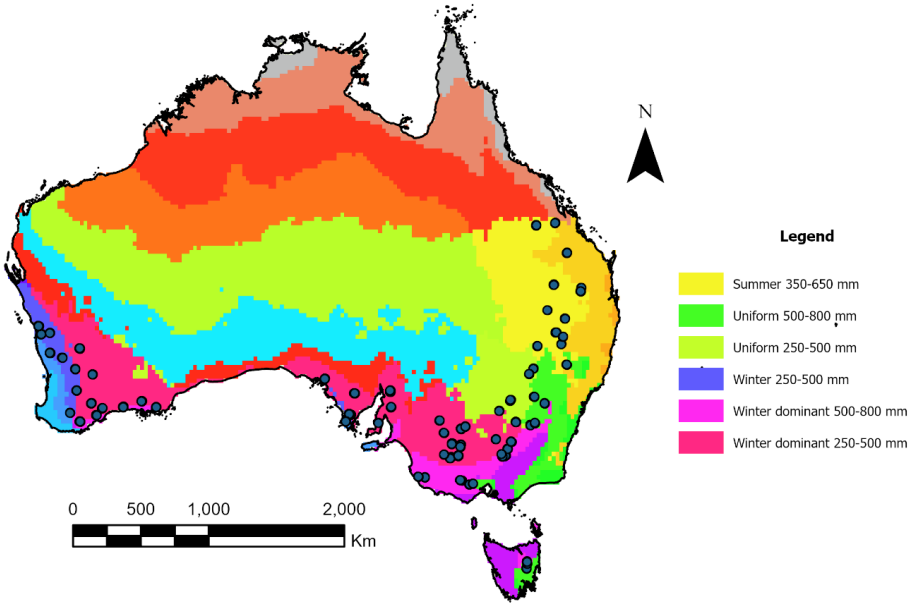

Figure 2: Location of study sites across Australia's major seasonal rainfall zones (1991–2020 climatology). Sites span six rainfall regimes, demonstrating the wide climatic range represented in the dataset. Data source: Australian Bureau of Meteorology (BOM).

Table 1: Classification of soil sample sites based on Australian Bureau of Meteorology (BOM) seasonal rainfall class

Classification ID	Soil sample sites	No. of farms	Rainfall region
1	324	13	Summer 350-650 mm
2	183	8	Uniform 500-800 mm
3	75	3	Uniform 250-500 mm
4	225	9	Winter 250-500 mm
5	300	12	Winter dominant 500-800 mm
6	675	27	Winter dominant 250-500 mm

2.3 Predictor variables

In this study, we considered six key soil properties: clay content, electrical conductivity (EC), cation exchange capacity (CEC), exchangeable sodium percentage (ESP), soil pH and silt+clay (the fine soil fraction, calculated as the sum of silt and clay) as predictors in the BLA model. The soil analysis was performed at four depth intervals (0-15 cm, 15-30 cm, 30-60 cm, 60-100 cm). We classified our data into two categories, topsoil and subsoil, to evaluate the depth-specific influence on SOC dynamics.

https://doi.org/10.5194/egusphere-2026-2466
Preprint. Discussion started: 20 May 2026

Topsoil is calculated as the mean of 0-15 and 15-30 cm intervals (0-30 cm), and subsoil, represented by the 30-60 cm interval. The topsoil layer generally reflects the processes that control SOC storage, which are regulated by texture, mineralogy, and aggregate protection. Subsoil is about processes that control plant growth and so impact on biomass production, which relates to biomass inputs into the topsoil. We created distinct BLA models for topsoil and subsoil predictors, utilising topsoil SOC (0–30 cm) as the response variable in both instances. This methodology enabled us to evaluate the impact of topsoil and subsoil properties on the attainable SOC levels in the upper 30 cm, the main area of concern for soil carbon sequestration and agricultural significance.

2.4 Calculation of attainable SOC using BLA

Despite the lack of a standard procedure for performing BLA, most studies use some or all of the following general steps (Shatar and McBratney, 2004; Makowski et al., 2007; Milne et al., 2006a; Patrignani et al., 2014; Lark and Milne, 2016; Hajjarpoor et al., 2018; Lark et al., 2020; Miti et al., 2024). The general steps which are adapted here include.

1. Compile data on measured SOC and related predictor variables (soil properties) throughout 72 farms, and subset by rainfall zone.
2. Select data points at each predictor that correspond to attainable SOC. This can be accomplished statistically or visually.
3. Fit a curve to the data chosen in the third step using a function which is the attainable SOC for the given value of the predictor variable.
4. Determine the SOC gap by subtracting the actual SOC from the attainable SOC determined in step 3.

In this study, a new BLA method (Al-Shammari et al., under revision) was used within each rainfall region (Table 1) to determine the attainable SOC and identify SOC limiting factors. This method integrates two denoising techniques in bivariate space, including Mahalanobis distance, which is used to identify and eliminate outliers from the point cloud, and the kernel density estimation (KDE) function, which is applied to select the points used for fitting the BL.

2.4.1 Data preprocessing and outliers' removal

Removal of outliers is a critical preprocessing step as it influences the reliability and quality of the BL fitting. In this study, outliers were identified and removed using the Mahalanobis distance (Equation 1), which involved calculating the distance for each point in the data cloud and subsequently grouping into small quantiles that increased from 0% to 100% in 2% increments.

$$D_M(x) = \sqrt{(x_i - \mu)^T \Sigma^{-1} (x_i - \mu)} \quad (1)$$

where $x_i = (\frac{x_i}{y_i})$ is the vector of predictor (x) and SOC (y) values for the i-th observation, μ is the mean vector, and Σ is the covariance matrix of the bivariate distribution.

The quantiles of the Mahalanobis distance were used to identify and eliminate the outliers. More specifically, observations with Mahalanobis distances exceeding the Qi-th percentile could be classified as outliers and subsequently removed from the analysis. This criterion can be expressed mathematically as:

Outlier = TRUE if $D_m > Q_i$; otherwise, Outlier = FALSE.

where $Q_{i\text{-th}}$ stands for the Mahalanobis distance distribution's percentile (98^{th} in this case). Outliers in this study were defined as points that fall within the top 2% percentile of the Mahalanobis distance values; thus, they were eliminated. This percentage, however, may be changed in light of local expertise and experience.

https://doi.org/10.5194/egusphere-2026-2466
Preprint. Discussion started: 20 May 2026

2.4.2 Kernel Density-Based Boundary Point Selection

Data points must be selected from the data cloud to represent the maximum attainable SOC to fit the BL. The most straightforward technique for selecting data points that represent the SOC potential at a specific predictor value is by looking at the data cloud. Nevertheless, this approach takes a lot of effort and time-consuming, particularly when dealing with big datasets. Therefore, statistical approaches can be more effective and appropriate for big datasets (Hajjarpoor et al., 2018). In this study, a multi-step statistical method was used to determine the main predictor values with their corresponding maximum SOC values. First, a 2-dimensional Kernel Density Estimation (KDE) approach was used to estimate the density values of the data points (both predictor and SOC) (Equation 2);

$$\hat{f}(x,y) = \frac{1}{nh_x h_y}\sum_{i=1}^{n} K\left(\frac{x-x_i}{h_x}\right)K\left(\frac{y-y_i}{h_y}\right), \quad (2)$$

where K is the kernel function, h_x and h_y are bandwidth parameters, and n denotes the total number of data points.

Following the computation of the density for each data point, the range of predictor values was divided into fifteen equal intervals. Predictor value segmentation was required to identify high and low-density data points within each interval. A moving window was used to extract points within ±1 bin width of each centre for each interval. The low-density data points could then be filtered out as they were not used in fitting the BL model, but retained in the data cloud. By excluding low-density data, the method becomes more targeted and less susceptible to random variation. Data points representing the SOC potential for each interval were then selected from the remaining points with higher densities to represent the attainable SOC for that interval. This method enabled us to filter points by density using a threshold, thereby determining how far the BL can be fitted from the denser points. The 95th percentile threshold was used in this study to find attainable SOC values. In particular, the top 95% of data points, based on their estimated density values, were retained within each bin, whereas the lowest 5% were excluded. From the remaining data in each interval, the highest SOC value was then chosen. The BL was then fitted using these attainable SOC values.

2.4.3 BL Fitting using LOESS

The final curve fitting to the BL has traditionally been performed manually. Afterwards, the statistical models employed were quartic polynomials (Schnug et al., 1995, 1996) and linear (straight-line) regression (Casanova et al., 1999). It may be feasible to more accurately depict SOC response shapes documented in the literature by using more flexible curves. In this study, a locally estimated scatterplot smoothing (LOESS) model was used to fit a set of boundary points (Cleveland and Devlin, 1988; Turicchi et al., 2020). LOESS regression is a non-parametric method that applies local polynomial models to a moving collection of data points without assuming anything about the data's structure (Turicchi et al., 2020). The method depends on a span, which is the percentage of points utilised for each local regression, to be determined. The range of permissible spans is 0 to 1, where bigger spans are usually utilised when fewer data points are available to ensure a smoother curve, while smaller spans result in closer fitting to the data and less smooth regression curves (Turicchi et al., 2020; Friedman, 1984).

2.5 Spatial modelling of soil properties at the case study farm

Twenty-five sites were analysed for every soil property (considered as predictors in the BLA model) at fixed depth intervals: 0-15 cm, 15-30 cm, 30-60 cm, and 60-100 cm. We then implemented a three-dimensional (3D) data-driven modelling strategy to map these soil properties throughout the soil profile. The 3D strategy seeks to account for the depth function of a given soil property within the profile by using the mid-depth of analysis as an explanatory variable (Filippi et al., 2019; Pozza et al., 2022; Tilse et al., 2022). Rather than traditional two-dimensional methods, which create separate models for each analysis depth interval, the 3D strategy allows us to develop a single model encompassing data from all depths. In this approach, a

https://doi.org/10.5194/egusphere-2026-2466
Preprint. Discussion started: 20 May 2026

mid-depth predictor was combined with selected spatial predictors (Table 2) in a random forest model (Breiman, 2001) to predict soil properties, such as organic carbon, in a single-step process that produces multiple digital soil maps at specified depths. Model performance was evaluated using multiple complementary metrics, including the concordance correlation coefficient (CCC), normalized Nash–Sutcliffe efficiency (NNSE), coefficient of determination (R^2), root mean square error (RMSE), and mean bias (Bias), providing a comprehensive assessment of agreement, predictive skill, variance explanation, error magnitude, and systematic bias.

As a whole, the modelling process occurs in the following steps: compile spatial soil and environmental predictors, perform model feature selection, fine-tune model parameters, validate the model and produce maps. Further details for each of these steps can be found in Wang et al. (2024). Given 25 sampling sites, leave-one-site-out cross-validation (LOSOCV) is performed iteratively, with all depths of a unique sample site 'left out' from model training for validation prediction during each iteration. The resulting validation predictions were combined to assess model performance. Rather than assessing validation predictions across the full dataset, it is essential to evaluate predictions at the original analysis depth intervals for sample sites to assess mapping quality at specified depths. Following validation, a 3D data cube of predicted digital soil maps for each analysis depth interval is produced. This is representative of predicted soil property (SOC, for example) across sampled fields and over the sampled 0-1 m soil profile of the farm. From this data cube, a composite topsoil layer (0–30 cm) was generated by averaging the 0-15 cm and 15-30 cm maps for the BLA model as predictor variables. A corresponding subsoil map (30–60 cm) was created for a separate subsoil BLA model, where subsoil properties were designated as predictors and topsoil SOC was modelled as the response variable.

Table 2: Selected predictors (along with mid-depth) utilised in the modelling.

Layer description	Layer type	Product details
Barest earth satellite imagery	Remote Sensing	30 m resolution - Geoscience Australia 30-year Landsat satellite imagery compilation of barest surface conditions - representative of long-term topsoil condition (Roberts et al., 2019).
Aerial radiometric map	Aerial gamma radiometrics	100 m resolution - Geoscience Australia radiometric map of Australia - shows airborne measured potassium, uranium and thorium (Minty et al., 2009).
Digital elevation map	Terrain attributes	30 m resolution - SRTM-derived (Shuttle Radar Topography Mission) 1-arcsecond digital elevation model (Gallant et al., 2011)
Soil landscape grid of Australia	Terrain attributes	30 m resolution - Soil and landscape grid of Australia derivative terrain covariates - slope (%), topographic wetness index (TWI), multi-resolution valley bottom flatness (MrVBF) (Grundy et al. 2015; Malone et al, 2025)
Electromagnetic survey	Proximal Sensing	10 m resolution - Interpolated proximal electromagnetic induction survey map
Radiometric survey	Proximal Sensing	10 m resolution - Interpolated proximal gamma radiometric survey map

https://doi.org/10.5194/egusphere-2026-2466
Preprint. Discussion started: 20 May 2026

2.6 Identification of the site-specific factors limiting SOC within a field of the case study farm

The above-mentioned steps are significant as they involve identifying the most limiting factors influencing the SOC accumulation and stabilisation for the case study farm. A multistep BLA approach was employed, adapted from the methodologies outlined by Shatar and McBratney (2004). Initially, boundary lines were applied to each predictor map created in the previous step to determine the maximum potential relationship between SOC and each individual soil property considered. These univariate BLA models indicate the maximum SOC that can be achieved for each soil property under current field conditions. This was followed by the construction of a multivariate BLA model using the von Liebig-type response framework suggested by Casanova et al. (1999). This model complies with Liebig's Law of the Minimum (Von Liebig, 1863), which states that the most limiting factor determines the attainable level of a response variable. We have adapted this model to find out the most limiting soil properties for achieving the maximum attainable SOC. Therefore, the minimum SOC value predicted by the individual boundary line functions across all soil properties was used to determine the attainable SOC for each sampling point in the study area. Using a multivariate BLA, it was possible to determine which soil property at each location was most limiting, or which factor contributed to the lowest expected attainable SOC value. The spatial distribution of these site-specific limiting factors was mapped to demonstrate within-field variation in attainable SOC storage.

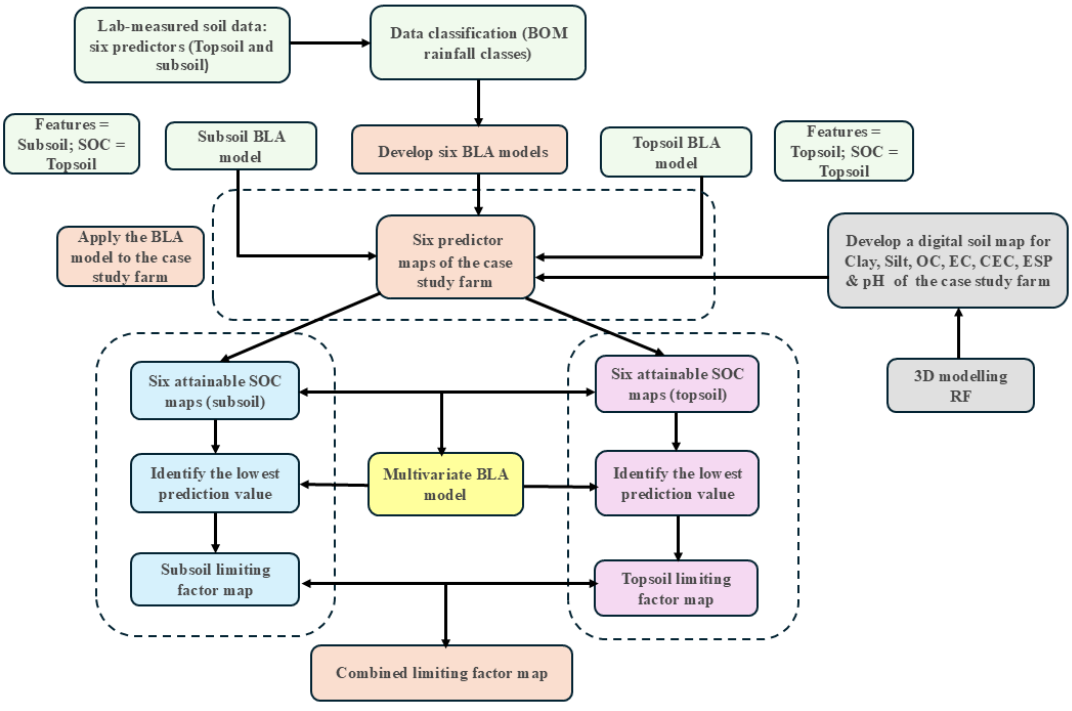

Figure 3: Methodological workflow for developing the Boundary Line Analysis (BLA) model and limiting factor maps

3. Results:

3.1 Attainable topsoil SOC (0-30 cm): Topsoil property-driven BLA

The results of the BLA are shown in Figure 4, categorised by six different rainfall regions for the topsoil (0-30 cm) layer. These results demonstrate the relationship between SOC and key soil properties, including clay, EC, CEC, ESP, pH and silt+clay. The laboratory-measured SOC values at the sampled sites are represented by the green scatter points, while the

https://doi.org/10.5194/egusphere-2026-2466
Preprint. Discussion started: 20 May 2026

boundary lines (black curves) generally indicate the attainable upper limit of SOC for specific values of each soil property, based on the best conditions captured in our dataset. The red points represent sample locations from the case study farm, which was used to create a digital soil map and subsequently to develop the limiting factor map. This shows that our case study farms fall in the Winter dominant 250-500 mm rainfall region.

Clay Content: Across all rainfall regions, a distinct quadratic pattern of the boundary line was observed with moderate clay contents (about 25-40 %) corresponding to the maximum attainable SOC levels (Fig. 4a) except the Summer 350-650 mm region, where the required clay content is 40-50 %. This implies that a moderate level of clay content in soil improves SOC storage capacity. Rainfall regions such as Winter dominant 500-800 mm and Uniform 500-800 mm showed the highest attainable SOC potential (approximately 2%) while Winter dominant 250-500 mm, Winter 250-500 mm and Summer 350 - 650 mm regions demonstrated comparatively lower attainable SOC sequestration potential, just above 1%. The other rainfall region, Uniform 250-500 mm, exhibited the lowest attainable SOC (~0.75 %).

EC: EC is a measure of soil salinity and shows a quadratic relationship with attainable SOC across the region; higher EC values correlate with lower attainable SOC. This might be due to elevated EC values, which impair plant growth, reduce microbial activity, and decrease biomass production. From Figure 4b, it is observed that an EC value ranging up to 0.3 dS/m is associated with high SOC sequestration, after which it declined. Rainfall regions with Winter dominant 500-800 mm exhibited the highest attainable SOC with a value of more than 2.5 %, and Uniform 500-800 mm exhibited the second highest attainable SOC (~1.75 %), while the other four regions showed a moderate level of attainable SOC, above and below 1 %.

CEC: Throughout the BOM rainfall regions, there were differences in the upper boundary line that described the relationship between SOC and CEC. The maximal attainable SOC was found to be highest in the Winter dominant 500-800 mm rainfall regions, representing an attainable SOC value of 2.5 %. The Uniform 500-800 mm also had a high SOC level (2 %). The lowest attainable SOC was observed in the Uniform 250-500 mm rainfall region. The other three regions demonstrated moderate attainable SOC potential, with values ranging from 0.9% to 1.2%. The maximum attainable SOC was determined from the higher CEC value (above 60 meq/100g), observed only in the Summer 350-650 mm region. The Winter dominant 500-800 mm and Uniform 500-800 mm regions showed the highest SOC potential, with CECs of 35-45 meq/100g. The other two regions exhibited that 20-30 meq/100g CEC yielded the maximum attainable SOC.

ESP: Across the majority of BOM rainfall regions, the upper boundary line revealed a continuous negative trend, suggesting that rising sodicity tends to limit SOC accumulation (Fig. 4d). The Winter dominant 500-800 mm and Uniform 500-800 mm regions had the largest attainable SOC potential, with the boundary line exceeding 2%. The Uniform 250-500 mm region, on the other hand, exhibited a lower attainable SOC (0.8 %), while the other three regions had more than 1 % attainable SOC. The highest attainable SOC remained at near-zero ESP in all BOM's rainfall regions.

Soil pH: The upper limit of the correlation between attainable SOC and soil pH depicted a clear quadratic trend across multiple rainfall regions, suggesting that there is an ideal pH range for SOC accumulation. SOC potential was found to be highest in the Winter dominant 500-800 mm region, where the peak of the boundary line was over 2.5 %. While the Uniform 500-800 mm showed an attainable SOC below 2%, the other four regions showed a value around 1%. The maximum attainable SOC was found in the pH range of 6.5 to 7.5 across almost all regions except the Uniform 500-800 mm. These areas demonstrated a clear link between SOC accumulation and near-neutral pH levels.

Silt+clay content (%): The shape of the boundary line from the silt+clay composite is nearly identical to that of clay alone. The largest attainable SOC was just above 2 %, which was observed in the Winter dominant 500-800 mm rainfall zone. The Uniform 500-800 mm region exhibited just below 2 % attainable SOC, while all other remaining BOM rainfall regions revealed a lower attainable SOC, varying from 0.75 % to below 1.5 %. It is also observed that 55-65 % of silt+clay yielded the highest attainable SOC in the summer 350-650 mm and 35-45 % of silt+clay required in the Winter 250-500. On the other hand, all four other regions showed attainable SOC peaking at 45-55 % of silt+clay.

https://doi.org/10.5194/egusphere-2026-2466
Preprint. Discussion started: 20 May 2026

Figure 5 compares the topsoil (0-30 cm) attainable SOC acquired from the BLA model with the measured SOC across the 72 grain growing farms, which are categorised by the six rainfall regions. Across all rainfall regions, attainable SOC consistently exceeded measured SOC, indicating a persistent SOC gap. The extent of this gap differs among the rainfall regions and among soil properties. It was also revealed that the measured SOC demonstrated narrower variability than attainable SOC in all soil properties.

Table 3 presents the statistics for topsoil measured SOC and attainable SOC (topsoil) across the dataset. It is observed that the mean measured SOC was 0.68 %, whereas the mean minimum attainable SOC was 0.98 % and the mean maximum attainable SOC was 1.39 %. The minimum attainable SOC (MinASOC) is the smallest BLA among the 6 predictors, and the maximum attainable SOC (MaxASOC) is the largest BLA among the 6 predictors. These MinASOC and MaxASOC were calculated for each location. All summary statistics showed the same pattern, suggesting a persistent gap between the measured SOC levels and their potential under ideal soil conditions. The observed SOC exhibited more relative variability (SD = 0.37) than the MinASOC (SD = 0.30), although variability was most pronounced for the MaxASOC estimates (SD = 0.46). The interquartile ranges revealed that the central 50% of observed SOC values ranged from 0.45 to 0.82%, whilst the ranges for the minimum and maximum achievable SOC were 0.78–1.08% and 1.12–1.83%, respectively.

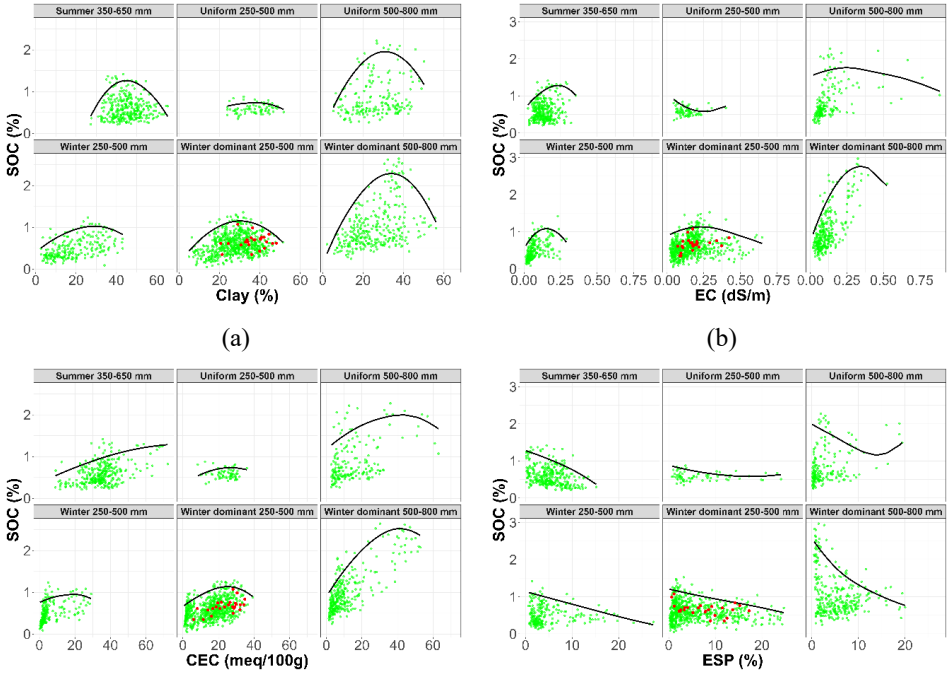

(a) (b)

(c) (d)

https://doi.org/10.5194/egusphere-2026-2466
Preprint. Discussion started: 20 May 2026

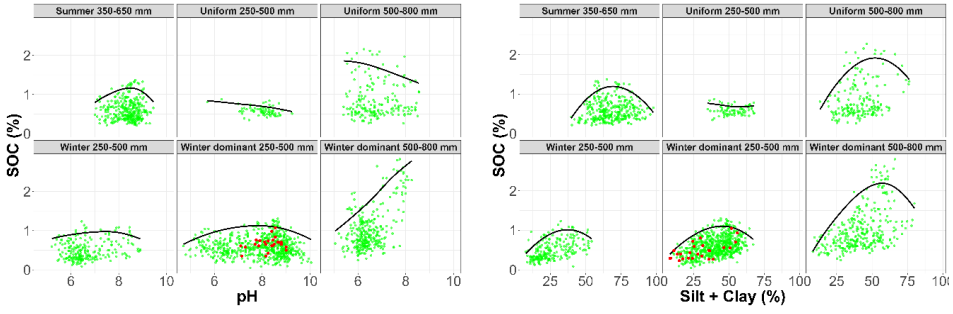

(e) (f)

Figure 4. Boundary line analysis (BLA) plots grouped by BOM seasonal rainfall class which illustrate the relationship between a) Clay content (%), b) Electrical Conductivity (EC) (ds/m), c) Cation Exchange Capacity (CEC) (milli-equivalents per 100 grams of soil), d) Exchangeable Sodium Percentage (ESP) (%), e) Soil pH, f) Silt+clay (%) and Soil Organic Carbon (SOC) (%) in topsoil (0-30 cm). The black line indicates the boundary line representing attainable SOC across six rainfall regions. The red discs represent the case study farm.

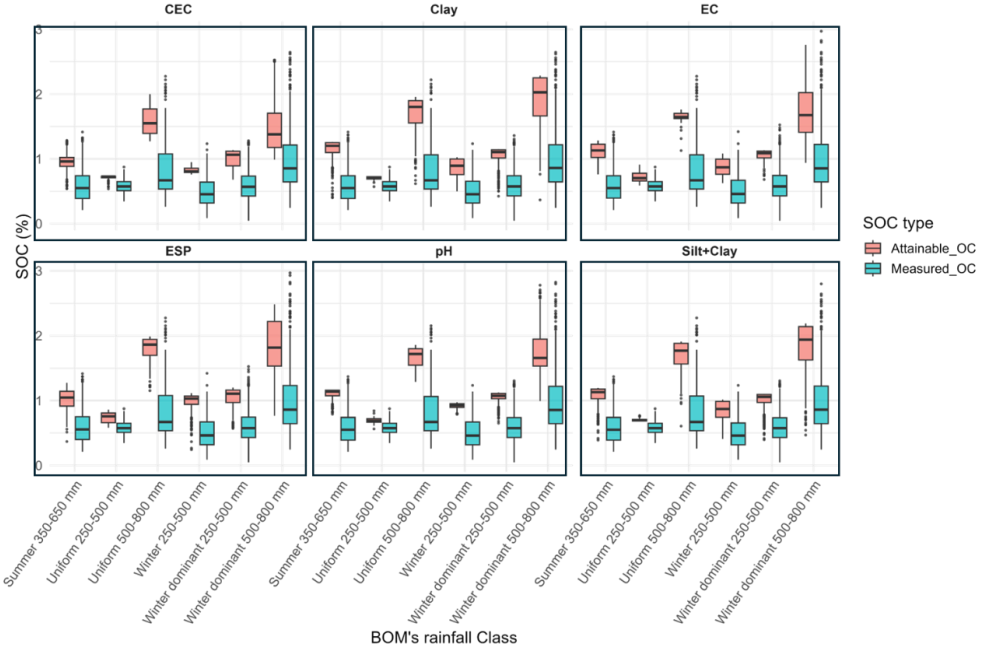

Figure 5. Attainable SOC vs measured SOC across the entire dataset, categorised by BOM's rainfall regions (topsoil property-based BLA)

https://doi.org/10.5194/egusphere-2026-2466
Preprint. Discussion started: 20 May 2026

Table 3. Descriptive statistics of observed SOC and attainable SOC (topsoil property-based BLA)

Statistic	Observed SOC (%)	Minimum attainable SOC (%) among all predictors	Maximum attainable SOC (%) among all predictors
Mean	0.68	0.98	1.39
SD	0.37	0.30	0.46
Median	0.61	0.94	1.17
Q1	0.45	0.78	1.12
Q3	0.82	1.08	1.83
Minimum	0.05	0.24	0.71
Maximum	2.65	2.19	2.78

3.2 Attainable topsoil SOC (0-30 cm): Subsoil-driven BLA

Similarly, we fitted the BLA model to subsoil (30-60 cm) properties to determine the topsoil attainable SOC, and Figure 6 illustrates the results of the boundary line, categorised by six different rainfall regions. These results also demonstrated the relationship between SOC and the same six key soil properties (clay, EC, CEC, pH, ESP and silt+clay content) for subsoil. The BLA plot's representation is the same as for the topsoil, indicating the upper limit of attainable SOC by the black boundary curve. In this case, the predictor variables were derived from the subsoil measurements (six key properties), whereas the response variable remained the SOC value of the topsoil (0-30 cm), enabling an evaluation of how deeper soil properties may affect carbon storing capability in the upper soil layer. This is likely to be due to the indirect effects of their impact on plant productivity and therefore biomass inputs, rather than direct impacts of stabilisation and decomposition, which are more relevant for the previous BLA based on topsoil properties.

Clay Content: Similar to the topsoil BLA model, a quadratic pattern of the boundary line was observed between SOC and clay across all rainfall regions (Figure 6a). The highest attainable SOC was found in two regions, such as Winter dominant 500-800 mm and Uniform 500-800 mm rainfall zones, reaching around 2.2 % and 1.75 % respectively at a clay content of 35-40%, while the Winter 250-500 mm and Winter dominant 250-500 mm regions showed comparatively lower attainable SOC, around 1 %, at 30-40 % of clay content level. The summer 350-650 mm region showed soil containing 40-50 % clay produced a moderate level of attainable SOC (1.25 %). The lowest attainable SOC was observed in the Uniform 250-500 mm region at 35-45 % clay content.

EC level: Panel 6b shows that there is a predominantly almost inverse correlation between EC and SOC across all BOM rainfall classes except Winter dominant 500-800 mm and Summer 350-650 mm zones. This means that attainable SOC potential declines with the increase of EC. In the regions such as Uniform 250-500 mm, Uniform 500-800 mm and Winter dominant 250-500 mm zones, the attainable SOC value began to decline at near-zero with the increase of EC. In the other three regions, attainable SOC decline started at EC level between 0.2 and 0.4 dS/m. The attainable SOC was found to be higher in the Winter dominant 500-800 mm (above 2.5 %) and Uniform 500-800 mm (2 %), while the other four regions showed a comparatively lower attainable SOC, ranging from 0.8 % to 1.1 %.

CEC: Across all rainfall regions, SOC and CEC illustrated a strong positive relationship, where higher CEC corresponds to higher attainable SOC (Figure 6c). The highest attainable SOC (2.5 %) was found in the Winter dominant 500-800 mm zone at 25 meq/100g CEC, while the lowest value (1.75 %) was reported in the Uniform 250-500 mm zones. The attainable SOC in the Uniform 500-800 mm, Winter 250-500 mm, Winter dominant 250-500 mm, and Summer 350-650 mm regions were 2.75 %, 1 %, 1.1 % and 1.25 % respectively, with the CEC level ranging from 20 meq/100g to 60 meq/100g. The findings are physiologically and chemically sound: soils with elevated CEC can retain more nutrients, hence enhancing plant production and organic matter contributions.

https://doi.org/10.5194/egusphere-2026-2466
Preprint. Discussion started: 20 May 2026

ESP: Throughout all rainfall regions, ESP exhibited a persistent negative correlation with SOC except in Uniform 500-800 mm, although the intensity and nature of this relationship vary across the rainfall regions. This implies that the attainable SOC decreases with the increase in ESP. The Uniform 500-800 mm exhibits a subtle positive curved pattern up to approximately 10 % ESP, which immediately declines. In the Winter dominant 500-800 mm region, where the highest attainable SOC was found (2.6 %), SOC decreases significantly as ESP rises, signifying that sodicity is a principal limitation. In the Winter 250-500 mm, Summer 350-650 mm and Winter dominant 250-500 mm regions, attainable SOC consistently decreases as ESP increases, with a moderate level of attainable SOC (around 1 %), with the impact being more pronounced at higher ESP levels. In contrast, Uniform 250-500 mm revealed a comparatively flatter curve with the lowest attainable SOC among the regions.

Soil pH: The boundary line is quite quadratic across the BOM's rainfall region, except Uniform 250-500 mm and Winter dominant 250-500 mm regions. The highest attainable SOC was observed in two regions, such as Uniform 500-800 mm and Winter dominant 500-800 mm (approximately 2 %), whereas the lowest SOC was found in the Uniform 250-500 mm (0.75 %). The other three regions revealed a moderate level of attainable SOC (above and below 1 %). A pH level of 7.5-8 showed the maximum attainable SOC in Uniform 500-800 mm and Winter dominant 500-800 mm, while the other four regions showed that soil with pH values above 8 has the potential for maximum attainable SOC.

Silt+clay content: The silt and clay composite also showed a positive and strong correlation with the attainable SOC potentials. An increased attainable SOC was found in high rainfall regions such as Winter dominant 500-800 mm, and Uniform 500-800 mm, representing 2.25 % and 1.75 % respectively. Other rainfall regions exhibited a moderate level of attainable SOC potential, except the Uniform 250-500 mm with 0.75 %, ranging from 0.9 to 1.2 %. It was also found that around 50-70 % of silt+clay content could yield increased attainable SOC across all the regions except the Winter 250-500 mm, which demonstrated that around 40 % silt+clay was enough for getting high attainable SOC.

Figure 7 contrasts the topsoil measured SOC across the 72 grain-growing farms, categorised by the six rainfall regions, with the topsoil (0-30 cm) attainable SOC obtained from the BLA model based on the subsoil (30-60 cm). There was a consistent SOC gap across all rainfall regions, with attainable SOC consistently exceeding measured SOC. The magnitude of this gap varies across different rainfall regions and soil properties. Additionally, the attainable SOC showed less variability than the measured SOC across all soil conditions.

Table 4 demonstrates the statistics for topsoil measured SOC and attainable SOC (topsoil) obtained from the BLA model based on subsoil properties as predictors. The mean observed SOC was 0.68%, whereas the mean MinASOC was 1.01 % and the mean MaxASOC was 1.39%. The pattern was consistent across all summary data, indicating a consistent gap between the current SOC levels and their potential in optimal soil conditions. The observed SOC showed a bit greater variability (SD = 0.37) than the MinASOC (SD = 0.31), although variability was highest at the MaxASOC estimates (SD = 0.52). The interquartile ranges were similar to those in Table 3: the central 50% of observed SOC values ranged from 0.45 to 0.82%, whilst the ranges for the minimum and maximum achievable SOC were 0.80–1.07% and 1.11–1.86%, respectively.

https://doi.org/10.5194/egusphere-2026-2466
Preprint. Discussion started: 20 May 2026

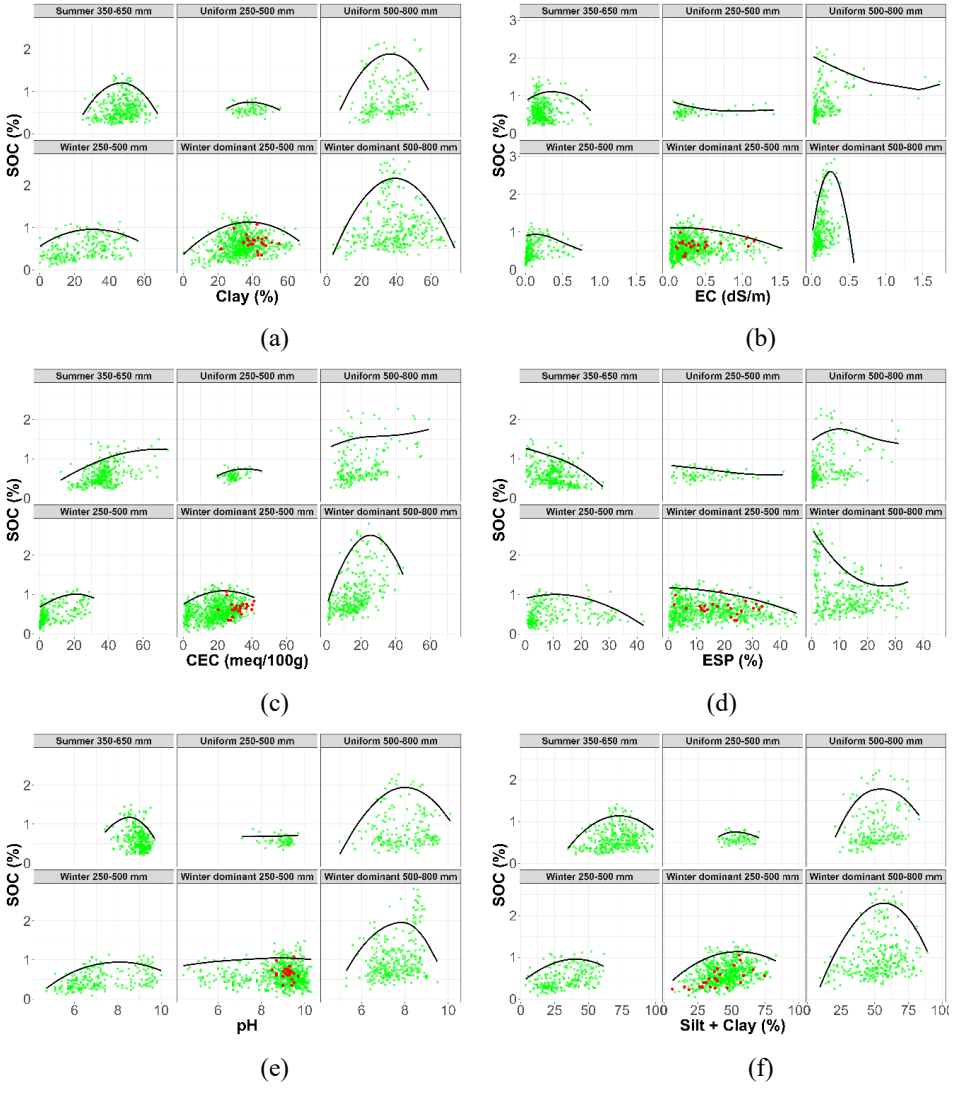

465

Figure 6. Boundary line analysis (BLA) plots grouped by BOM seasonal rainfall region which illustrate the relationship between a) Clay content (%), b) Electrical Conductivity (EC) (ds/m), c) Cation Exchange Capacity (CEC) (milli-equivalents per 100 grams of soil), d) Exchangeable Sodium Percentage (ESP) (%), e) Soil pH, f) Silt+clay (%) of subsoil and Soil Organic Carbon (SOC) (%) in topsoil. The black line indicates the boundary line representing attainable SOC
470 **across six rainfall regions. The red discs represent the case study farm.**

https://doi.org/10.5194/egusphere-2026-2466
Preprint. Discussion started: 20 May 2026

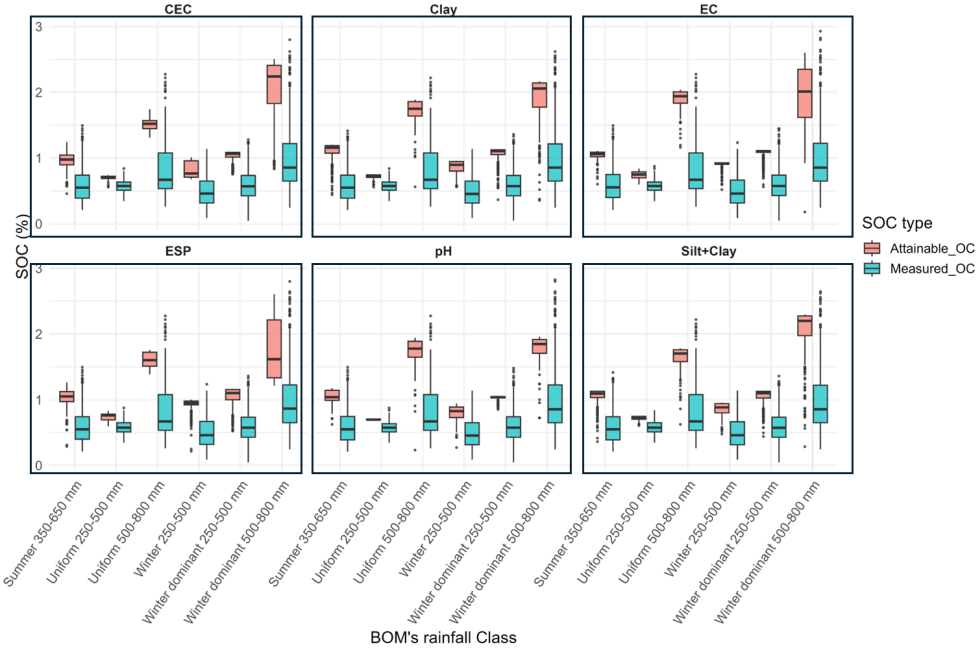

Figure 7. Attainable SOC vs measured SOC across the entire dataset, categorised by BOM's rainfall class (subsoil property-based BLA)

Table 4. Descriptive statistics of observed SOC and attainable SOC (subsoil property-based BLA)

Statistic	Observed SOC (%)	Minimum attainable SOC (%) among all predictors	Maximum attainable SOC (%) among all predictors
Mean	0.68	1.01	1.39
SD	0.37	0.31	0.52
Median	0.61	0.97	1.15
1st quartile (Q1)	0.45	0.80	1.11
3rd quartile (Q3)	0.82	1.07	1.86
Minimum	0.05	0.18	0.71
Maximum	2.62	1.96	2.61

3.3 Digital Soil mapping of the soil properties (predictors) of the case study farm

The spatial distribution of key topsoil properties, including clay content, EC, CEC, ESP, pH and silt+clay of the case study farm, is depicted in Fig. 8. These digital soil maps are derived from laboratory-analysed soil samples obtained from the topsoil layer (0-30 cm). In addition, subsoil maps (30-60 cm) of these soil properties of the case study farm were also developed to employ the BLA model to estimate topsoil attainable SOC. Topsoil properties maps are shown for illustration here, and subsoil maps are provided in Annex 1. From Figure 8, distinct spatial variability is evident throughout the case study farm, emphasising regions with differing soil properties. The clay percentage exhibited variability across the farm, ranging from around 24% to 45%. The map demonstrates significant spatial variation, with elevated clay content mostly in the northern and southern regions of the farm, whilst the central areas displayed comparatively lower clay levels. From panel 8b, the EC content ranges from 0 to 0.6 dS/m, with some variability across the region, while the north region showed higher EC, and the central zone had significantly lower EC. CEC content ranges from 7 to 35 meq/100g, and most of the regions' soil had large values of CEC, particularly the northern and southern regions with increased CEC, and the central zone had remarkably lower CEC (Panel

https://doi.org/10.5194/egusphere-2026-2466
Preprint. Discussion started: 20 May 2026

8c). In terms of ESP content of soil, most of the farm soil had low ESP (0-10 %), and the northern part had high ESP, which was above 10 % (Panel 8d). Soil pH ranges from 7.2 to 8.6, with a greater variation throughout the farm, demonstrating elevated pH in the southern region of the field. Silt+clay represents the summation of clay and silt content. It was observed that, except for the central zone, the entire study was enriched with silt+clay content with a variation ranging from 32 to 62 %. The textural class of this case study firm soil is mostly clay loam to clay, and grey to grey- brown in colour and also belongs to the Vertosol soil order (Isbell, 2002). This spatial variability in various soil properties could be the result of the parent material, the elevation of the landscape, and soil intervention for crop production. Understanding the distribution of these soil properties is crucial for evaluating soil organic carbon, recognising potential limitations to crop yield and carbon storage, and directing site-specific soil management approaches.

Table 5 demonstrated that Random Forest (RF) models had different levels of predictive performance across different soil properties and depths. Overall, the model demonstrated moderate to high accuracy for soil organic carbon and certain chemical parameters. However, textural properties showed relatively inferior performance, especially in deeper layers. The accuracy of predicting SOC was consistently moderately good across all layers (CCC = 0.64–0.74, NNSE = 0.68-0.74), and almost no bias. Textural qualities such as clay and silt typically showed higher prediction errors and were predicted with low to moderate accuracy, with CCC ranging from 0.16 - 0.48 and NNSE ranging from 0.50 – 0.60, especially at intermediate depths (CCC = 0.16-0.32 and NNSE = 0.50-0.53). EC attained CCC values between 0.62 and 0.69, with NNSE ranging from 0.56 to 0.71, showing higher performance at the 30-60 cm depth range while maintaining consistently low bias across depths. CEC exhibited the most robust surface-layer performance (CCC = 0.84; NNSE = 0.83 at 0–15 cm), with diminished performance at increased depths. The prediction of pH was very poor at the top layer (CCC = 0.28; NNSE = 0.47) but significantly enhanced at depths of 15–30 cm (CCC = 0.67; NNSE = 0.66) and 30–60 cm (CCC and NNSE = 0.62). The ESP model showed a moderate predictive performance throughout all layers, with increasing accuracy at higher depth.

Table 5. Modelling performance metrics on validation data.

Soil property	Depth (cm)	CCC	R^2	NNSE	Bias	RMSE
SOC	0-15	0.74	0.64	0.74	0.00	0.12 %
	15-30	0.64	0.52	0.68	-0.01	0.11 %
	30-60	0.71	0.58	0.71	0.01	0.07 %
Clay	0-15	0.48	0.31	0.60	0.72	5.19 %
	15-30	0.16	0.01	0.50	0.78	10.53 %
	30-60	0.38	0.22	0.57	-0.80	6.01 %
Silt	0-15	0.40	0.23	0.57	-0.19	3.23 %
	15-30	0.32	0.16	0.53	1.26	4.26 %
	30-60	0.28	0.10	0.53	-0.15	4.22 %
EC	0-15	0.64	0.47	0.56	0.02	0.06 dS/m
	15-30	0.62	0.44	0.65	0.01	0.10 dS/m
	30-60	0.69	0.57	0.71	0.01	0.23 dS/m
CEC	0-15	0.84	0.81	0.83	1.11	4.34 meq/100g
	15-30	0.68	0.56	0.70	0.18	5.76 meq/100g
	30-60	0.42	0.23	0.57	-0.61	4.71 meq/100g
pH	0-15	0.28	0.05	0.47	-0.01	0.62
	15-30	0.67	0.48	0.66	-0.01	0.30
	30-60	0.62	0.40	0.62	0.00	0.23
ESP	0-15	0.47	0.28	0.55	1.22	3.33 %
	15-30	0.55	0.44	0.64	-0.20	5.33 %
	30-60	0.56	0.40	0.63	1.24	7.50 %

https://doi.org/10.5194/egusphere-2026-2466
Preprint. Discussion started: 20 May 2026

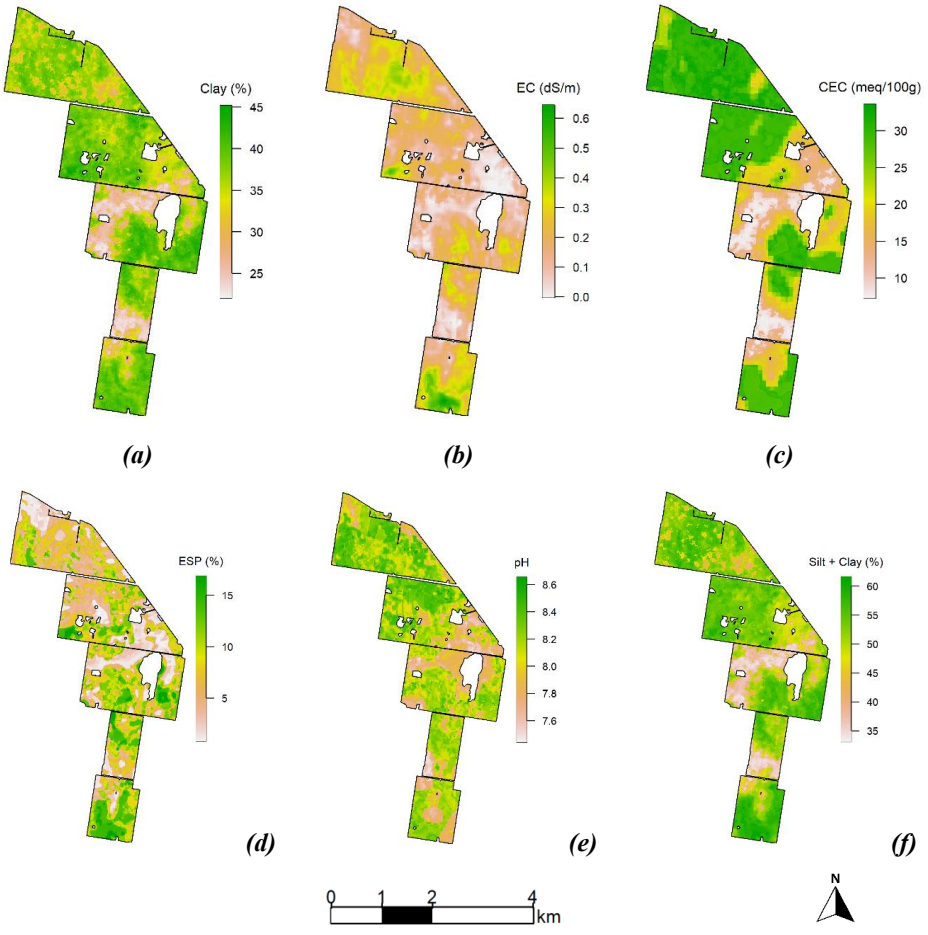

Figure 8: Digital soil maps of laboratory-measured key soil properties of case study farm (Topsoil): (a) Clay content, (b) Electrical Conductivity (EC), (c) Cation Exchange Capacity (CEC), (d) Exchangeable Sodium Percentage (ESP), (e) Soil pH, (f) Silt+clay content

Attainable SOC from soil properties is estimated by implementing the BLA prediction, which denotes the anticipated maximum attainable SOC content derived from the model between SOC and soil properties through the BLA methodology. This method determines the maximum attainable SOC at a specified soil property value (e.g. EC), under existing field conditions, accurately reflecting the perfect scenario in which EC is the sole constraint. We applied the developed BLA prediction model to the case study farm, which falls under the Winter dominant 250-500 mm rainfall region as indicated by the red points (Fig. 4), using specific key soil properties as predictors in order to illustrate how the BLA is used for assessing attainable SOC. Different patterns of attainable SOC were observed across the farm in the spatial prediction maps produced for clay content, EC, CEC, ESP, soil pH and silt+clay.

The anticipated attainable SOC levels were consistently higher in areas with a moderate level of clay content (Fig. 9a), especially in the central zones. This aligns with clay's established function of stabilising organic materials at a moderate level by forming microaggregates and fostering robust organo-mineral relationships. The EC-based SOC map (Fig. 9b) showed that, except for some parts of the northern and southern regions, there is a high attainable SOC distribution across the farm. This reflects that the very low level of salinity is favourable for fertility conditions that support microbial activity and plant growth

https://doi.org/10.5194/egusphere-2026-2466
Preprint. Discussion started: 20 May 2026

and lead to SOC accumulation. The range of attainable SOC across the farm was found to be narrower in the CEC-based map (Fig. 9c); the value remained low in the northern region (0.8-0.85 %), whereas the remaining regions mostly had around 0.9 %. A wide range of attainable SOC (from around 0.6 % to about 1.1 %) was also shown by ESP-based estimation (Fig. 9d), where the northern and central regions demonstrate higher attainable SOC compared to the southern region. The map recognised sodicity as a major limitation, resulting in diminished attainable SOC potential in sodic areas (higher ESP) due to inadequate soil structure, impaired aeration, and restricted microbial activity. The pH-based attainable SOC map (Fig. 9e) indicated significant spatial heterogeneity, with greater SOC anticipated in soils exhibiting near-neutral to slightly alkaline pH values, implying that high pH levels may hinder microbial processes critical to carbon cycling. Finally, the silt+clay exhibited the attainable SOC ranged from 0.8 % to more than 1 % with higher SOC found in the central zone (Fig. 9f). Interestingly, the value of attainable SOC was higher in the region where the value of silt+clay is around 30-40 % and lower SOC in the area with higher silt+clay (above 50 %). The reason for the higher silt+clay connected to lower SOC might be that soil with higher silt+clay content may be compacted with poor soil structure, reduced aeration, which limits plant root growth, impairs microbial activity and lowers SOC input. These spatial maps collectively illustrate how the BLA may delineate the impact of specific soil properties and underscore both the potential and constraints for increasing SOC at the farm level. This method has the potential to enhance precision soil management and facilitate focused interventions, such as sodic soil amelioration, pH modification through liming and organic amendments in low-potential areas to advance sustainable soil carbon management in agricultural systems.

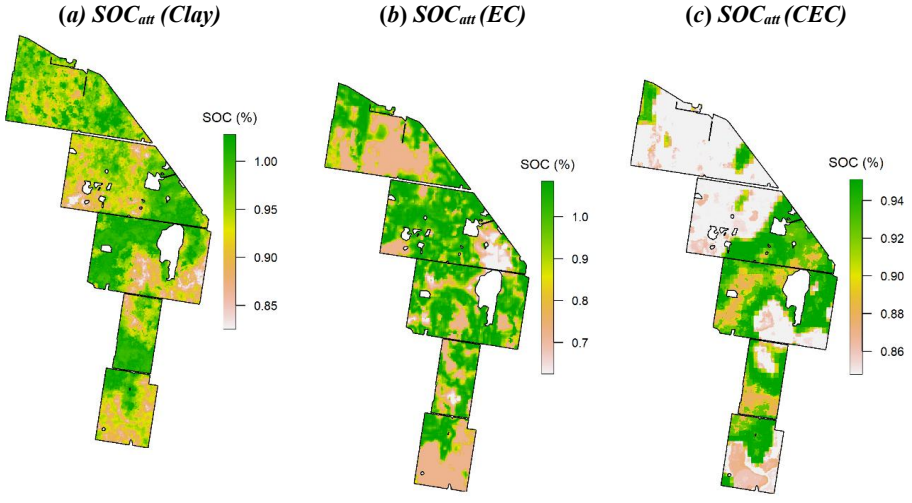

https://doi.org/10.5194/egusphere-2026-2466
Preprint. Discussion started: 20 May 2026

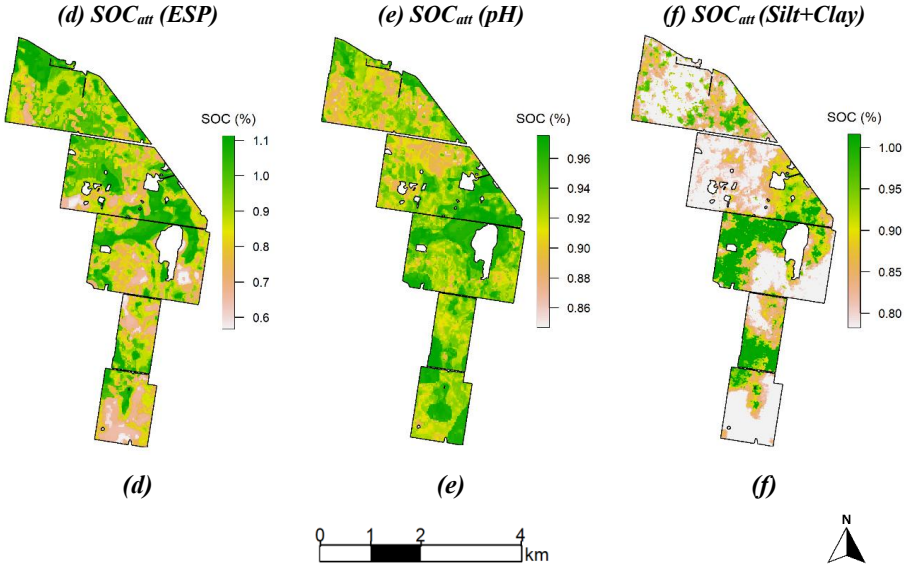

Figure 9. Attainable topsoil SOC (0-30 cm) as a function of key topsoil properties using Boundary Line Analysis (BLA): (a) Clay content, (b) Electrical Conductivity (EC), (c) Cation Exchange Capacity (CEC), (d) Exchangeable Sodium Percentage (ESP), (e) Soil pH, (f) Silt+clay content

Figure 10 illustrates a series of spatial maps that apply the BLA model to detect and possibly alleviate soil constraints that limit SOC buildup at the farm level. Panel 10a illustrates the minimum attainable SOC, obtained by identifying the lowest predicted SOC value from six distinct BLA models, which are based on six key soil characteristics: clay content, EC, CEC, ESP, pH, and silt+clay content. This predicted minimum value denotes the most limiting condition for SOC accumulation at each site, which is linked to the principle of the law of minimum. Subsequently, a spatial map (Fig. 10b) was created based on soil properties associated with the lowest predicted value. This map is referred to as a limiting factor map for SOC accumulation. This illustrates the soil properties in relation to the degree of constraint on building SOC and productivity. This map provides critical information on which soil properties constrain SOC accumulation and, in which locations on the farm, these constraints occur. From Figure 10b and Table 6, it is observed that EC, ESP and silt+clay are the most dominant limiting factors throughout the farm, affecting 25.12 %, 32.86 % and 33.72 % of the area, respectively. This information enables farmers to take appropriate soil measurements to ameliorate these limiting properties to increase SOC levels. Panel 10c is an example case where the utilisation of this diagnostic method in a management setting is demonstrated by simulating a scenario in which the ESP constraint has been completely mitigated, for instance, through the application of gypsum - a common amelioration technique for sodic soils. The generated map illustrates the potential increases in SOC levels via targeted ESP management, especially in locations of the farm that were previously affected by high ESP. By quantifying the SOC gain, Panel 10d illustrates the regions where the SOC sequestration would be greatest following sodicity amelioration.

https://doi.org/10.5194/egusphere-2026-2466
Preprint. Discussion started: 20 May 2026

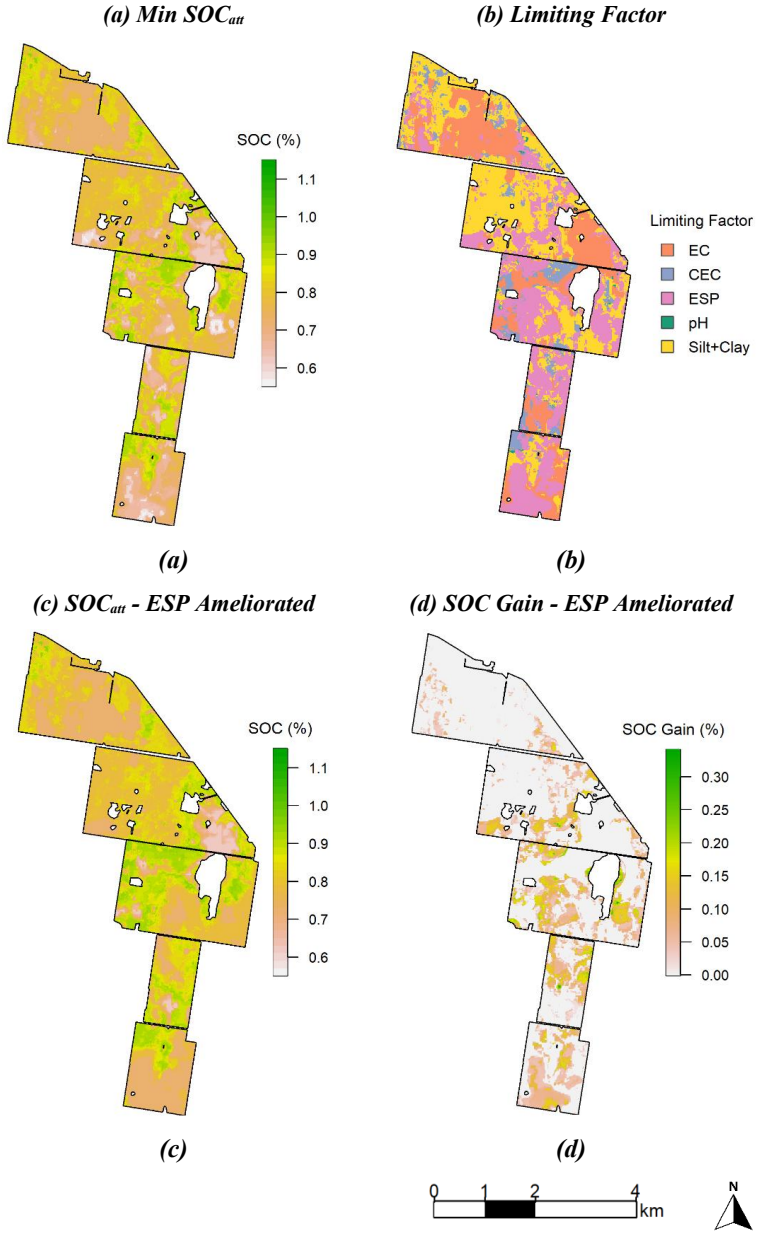

580 **Figure 10. (a) Minimum attainable SOC from all six BLA predictions (topsoil); (b) Limiting factor map (topsoil); (c) Attainable SOC after ameliorating exchangeable sodium percentage (ESP) constraint (topsoil); (d) Attainable SOC gain after ameliorating ESP (topsoil)**

585

https://doi.org/10.5194/egusphere-2026-2466
Preprint. Discussion started: 20 May 2026

Table 6: Proportion of total area of case study farm impacted by soil properties identified as the most limiting factor in the topsoil (0-30 cm).

590

Limiting Factor	*Area (%)*
EC	25.12
CEC	7.99
ESP	32.86
pH	0.31
Silt+clay	33.72

Following the concept of applying the BLA model to a case study farm, which was previously employed for the topsoil as illustrated in Figure 9, we also developed the BLA model based on the soil measurement data of the subsoil layer (30-60 cm). We determined the upper envelope of topsoil's attainable SOC as a function of key properties of subsoil (Fig. 11). We applied this subsoil-derived model to create a spatial map of attainable SOC and determine the limiting factor for the topsoil SOC for the case study farm. The attainable SOC as a function of clay varies from 0.85 to 0.96 % throughout the case study farm, which is less compared to topsoil, while the majority of the area has more than 0.90 % of attainable SOC (Fig. 11a). A wide range of attainable SOC was observed (0.6 to 0.95 %) based on the EC prediction (Fig. 11b) across the farm, while majority of the farm had higher values, more than 0.85 %. The CEC-based attainable SOC prediction map shows SOC values ranging from 0.85 % to more than 1 % across the farm area. The northern part had the patches containing comparatively lower SOC than the central and southern regions (Fig. 11c). Across the farm, the value of attainable SOC as a function of ESP falls within a limited range, from 0.90 to 1 % (Fig. 11d). Apart from some patches in the central zone and north corner, attainable SOC was observed at above 0.96 %. From Figure 11e, representing the attainable SOC prediction map based on the soil pH, a high SOC (0.94 %) was observed almost uniformly across the entire farm, indicating that subsoil pH is almost uniformly distributed throughout the region. Compared with clay alone, the estimated attainable SOC as a function of the silt + clay composite was slightly lower; however, it still followed the same spatial pattern, with the highest value in the central region.

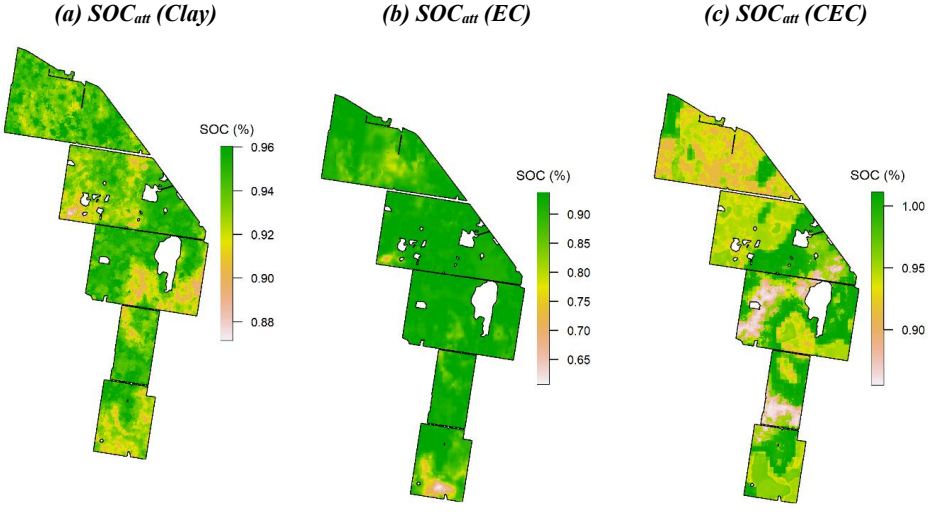

https://doi.org/10.5194/egusphere-2026-2466
Preprint. Discussion started: 20 May 2026

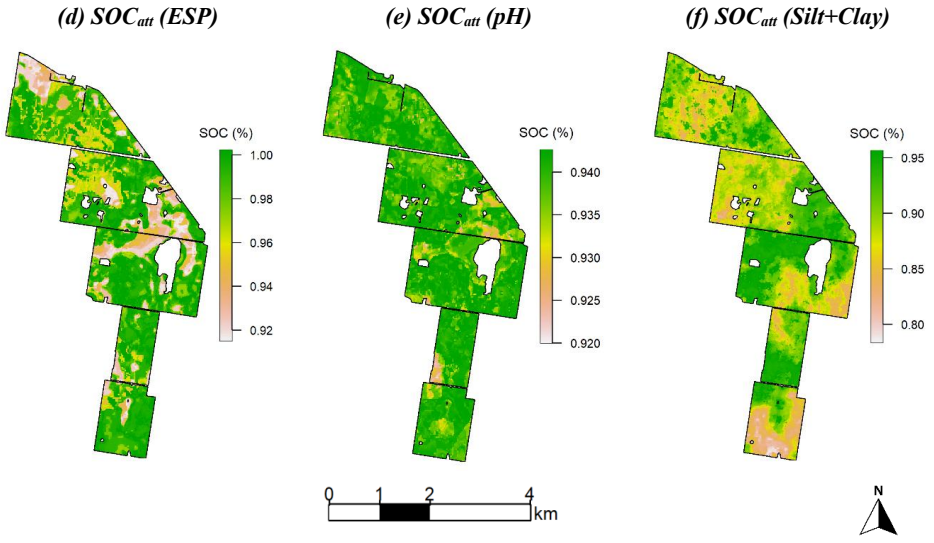

610 **Figure 11. Attainable topsoil SOC (0-30 cm) as a function of key subsoil properties using Boundary Line Analysis (BLA): (a) Clay content, (b) Electrical Conductivity (EC), (c) Cation Exchange Capacity (CEC), (d) Exchangeable Sodium Percentage (ESP), (e) Soil pH, (f) Silt+clay content**

A subsoil limiting factor map (Fig. 12a) was produced by employing the multivariate BLA model, which was built on the
615 subsoil dataset, using the principle of the law of minimum. Specifically, for each location, we identified the lowest predicted SOC value obtained from the BLA models in relation to specific soil variables (e.g., clay, EC, CEC, ESP, pH, and silt+clay) and designated the associated soil property as the most limiting factor. The main limiting factor for SOC accumulation across the case study farm is silt+clay, representing 61.3 % of the area (Table 7), which is evident as shown in Figure 12a. The second-most limiting factor is EC, representing 26.27 % of the total area affected in SOC accumulation. The EC constraint exists in
620 some parts of the northern, central and southern areas. In the central region, there is a combination of patches of silt+clay, CEC and EC as the limiting factors. However, the SOC gains if these subsoil limiting factors are removed were not illustrated (similar to Figure 10c for topsoil) because soil amelioration is very hard, and mostly impossible at depth.

In the final phase, we integrated the separate limiting factor maps for the topsoil and subsoil layers to produce a combined limiting factor map (fig. 12b). This integrated method recognises that soil constraints on SOC accumulation can differ
625 significantly across layers and are not limited to a particular depth. The combined map identifies the most limiting soil property for each site across both layers using the law of minimal principles. This offers a more comprehensive and agronomically applicable perspective on soil constraints. Figure 12b, representing the combined limiting factor map, where it is clearly evident that the silt+clay content of topsoil is the most dominant limiting factor throughout the farm, representing 33.5 % of the entire area (Table 8). ESP of the topsoil stands for the 2nd most limiting factor, reflecting that 32.3 % of the farm area was affected
630 by the high sodicity (Table 8). EC of topsoil was also found to be the most significant soil constraint that potentially limits the SOC accumulation for the 24.9 % area of the case study farm. All other limiting factors, such as subsoil EC, CEC, ESP, pH and topsoil CEC and pH, comprised the remaining 9.3 % of the area. The central zone of the farm is dominated by patches of EC and ESP of topsoil, while the northern region is highly affected by EC and silt+clay of topsoil.

635

https://doi.org/10.5194/egusphere-2026-2466
Preprint. Discussion started: 20 May 2026

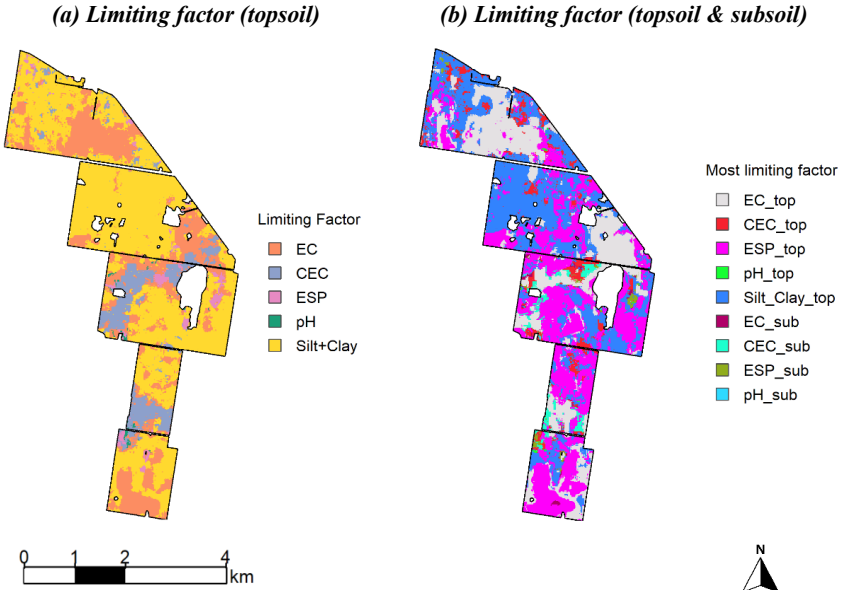

Figure 12. (a) Limiting factor map for subsoil; (b) Limiting factor map (topsoil and subsoil)

Table 7: Proportion of total area of case study farm impacted by subsoil properties (30-60 cm) identified as the most limiting factor on topsoil SOC accumulation.

Limiting Factor	*Area (%)*
EC	26.27
CEC	9.57
ESP	2.45
pH	0.41
Silt+clay	61.3

Table 8: Proportion of total area of the case study farm impacted by topsoil and subsoil properties identified as the most limiting factor on topsoil SOC accumulation.

Limiting Factor	*Area (%)*
EC top	24.9
EC sub	0.61
CEC top	5.43
CEC sub	2.12
ESP top	32.3
ESP sub	0.74
pH top	0.20
pH sub	0.09
Silt+clay top	33.5

https://doi.org/10.5194/egusphere-2026-2466
Preprint. Discussion started: 20 May 2026

4. Discussion

4.1 BLA modelling at the regional scale

This study demonstrates that the BLA framework is highly effective for estimating attainable SOC in relation to various soil properties across the grain region of Australia. Although different methods in estimating attainable SOC, including linear regression, have been used in previous studies, Feng et al. (2013) reported that BLA estimated more than twice the maximum organic carbon storage than linear regression, suggesting that linear regression was insufficient for such predictions. Since then, a number of researchers, such as Beare et al. (2014), Fujisaki et al. (2018), Wenzel et al. (2022), and Jien et al. (2025), have utilised a BLA model across diverse agroecosystems to estimate attainable SOC potential. Lark and Milne (2016) applied the BLA model to estimate nitrous oxide (N_2O) emissions from soil as a function of several soil characteristics. More recently, Jien et al. (2025) also demonstrated that the BLA estimated SOC sequestration potential was 2.1 times higher than that of quantile regression, reinforcing the suitability of the BLA model in determining SOC.

In our analysis, the attainable SOC across the grain regions of Australia in the topsoil (0-30 cm) varied from 0.98 % (mean minimum) to 1.39 % (mean maximum), whereas the average actual (measured) SOC was 0.68 % (SD = 0.37; IQR = 0.45 - 0.82) (Tables 3 & 4). This gap underscores a significant potential for SOC sequestration in the topsoil, with possible enhancements ranging from 0.30 % to 0.71 %, depending on rainfall zones and management strategies. In contrast, the attainable topsoil SOC derived from the subsoil-based BLA model was calculated to be 1.01 % (mean minimum) -1.39% (mean maximum), indicating a further sequestration potential of 0.33-0.71%. These findings highlight that although topsoil properties hold the greatest potential for SOC storage, subsoil physical and chemical properties also contribute significantly to long-term SOC sequestration, demonstrating how deeper soil layers control topsoil carbon stabilisation. Figures 5 and 7 demonstrate that the magnitude of potential SOC sequestration varies among rainfall regions and soil properties, as indicated by SOC gaps, which are defined by the difference between the observed and attainable SOC.

Based on the six BLA models in relation to all six soil key properties, it is evident that the maximum attainable SOC is significantly varied among all rainfall zones. This is because rainfall has a great impact on the pedogenic process, as well as different soil physical and chemical properties. It is known that climate, which includes temperature and precipitation, is a primary driver of SOC (Jenny, 2012; Bui et al., 2009; Minasny et al., 2013; Viscarra Rossel et al., 2014; Hobley et al., 2015). Soil moisture can alter the composition of the soil microbial community and nutrient availability (Franzluebbers et al., 1994; Meisner et al., 2013; Drenovsky et al., 2010; Brockett et al., 2012; Cavagnaro, 2016). Orgill et al. (2017) found that higher SOC stocks in Australian soil are highly linked with higher summer and spring rainfall. They also showed that parent material influenced the SOC fraction stock in the 0-30 cm soil layer within a climatic zone. Overall, our results demonstrated that the Uniform 500-800 mm region and the winter dominant 500-800 mm region exhibit the greatest SOC sequestration potential across all evaluated soil properties, representing broadly eastern-southern and western Australia, respectively.

The study shows that clay content is a critical factor for potential SOC sequestration. Xu et al. (2016) demonstrated that clay minerals played a major role in controlling SOC accumulations in regions with high rainfall. The BLA model based on both topsoil and subsoil properties revealed that the ideal clay content for maximising topsoil SOC accumulation is around 30-60%, after which attainable SOC declines. The reason might be that high clay content makes soil more susceptible to compaction, reducing porosity, water infiltration, microbial activity, nutrient cycling, and hindering root growth (Ogorek et al., 2025). In the BLA model with EC, a convex upper boundary envelope was observed in the Uniform 250-500 mm and Uniform 500-800 mm zones in the subsoil. This implies that attainable SOC increases as EC increases, which seems contradictory because higher EC levels are typically associated with soil constraints. Additionally, ESP showed a similar convex curve in those regions, which is not commonly reported in relation to SOC accumulation. The reason may be the co-occurrence of significant clay content in these areas, or there are scarce or unrepresentative data points in these particular zones, which require careful interpretation. With regard to pH, topsoil exhibited almost a flat BL line, and subsoil showed a quadratic curve in these regions. Other regions followed a similar boundary line for topsoil. Across all rainfall regions, attainable SOC is found to be higher in

https://doi.org/10.5194/egusphere-2026-2466
Preprint. Discussion started: 20 May 2026

the topsoil compared to the model built on the subsurface soil in all soil properties. This is expected as topsoil receives direct organic matter such as plant residue, litterfall, organic compost and microbial activity, which are the precursors of the accumulation of SOC (Clara et al., 2017) and decrease microbial activities in the subsoil (Preusser et al., 2017). However, subsoil properties contribute indirectly to topsoil SOC through their influence on plant growth and biomass production, which controls the amount of organic inputs returned to the surface. In this way, subsoil serves as a supporting layer that regulates the availability of water and nutrients, which in turn controls aboveground productivity and subsequent carbon inputs to the topsoil. As a result, whereas SOC accumulation mostly takes place in the topsoil, subsoil limitations on carbon inputs from plants also play a role.

4.2 BLA implementation to identify limiting factors at the farm scale

Based on the multivariate BLA model, the generated limiting factor maps offer a precise and quantitative framework for determining the main soil constraints controlling SOC buildup throughout the case study farm. The topsoil limiting factor map revealed that EC, ESP, and silt+clay were equally distributed soil constraints, suggesting that multiple topsoil properties jointly control SOC dynamics. The subsoil limiting factor map, on the other hand, showed a more distinct pattern, with silt+clay appearing as the dominant limiting factor across approximately two-thirds of the farm, while EC accounted for the majority of the remaining constrained area. However, interpretation based solely on topsoil or subsoil maps is inadequate for determining the dominant, profile-scale constraint or for planning efficient, whole-farm soil management strategies, as SOC accumulation reflects the combined influence of both surface and subsurface soil conditions. To solve this, a map of combined limiting factors was created to determine which soil layer at each site ultimately controls the attainable SOC.

Interestingly, the topsoil pattern was mainly reflected in the combined limiting factor map, suggesting that surface soil conditions are the primary driver of SOC restrictions as compared to the subsoil. This emphasises how important topsoil characteristics are in determining SOC accumulation and stability across the farm, especially sodicity, salinity, and texture. This is probably because these properties have a significant impact on root formation, water retention, and the stabilisation of organic matter over the long term. Among the identified constraints, ESP was found to be one of the most significant soil constraints for the SOC buildup across the farm, affecting around one-third of the farm (32.3 %). This offers a clear and implementable guideline for soil management. By applying gypsum fertiliser to the ESP-constrained site of the farm, for example, a more optimum ESP range can be restored, improving microbial activity and the environment for SOC buildup (Roberton et al., 2020). This outcome demonstrates a significant potential for carbon sequestration through sodicity management. In addition to ESP, EC and silt+clay are also the major soil constraints across the farm. Elevated EC indicates high salinity in soil, which can restrict SOC accumulation by inhibiting plant growth and microbial activity. It would be very difficult to manage soil salinity in a dryland agriculture system in Australia. However, silt+clay factor can be managed to a great extent by adding organic inputs such as cover crops, stubble retention, compost manure or other agronomic management. In addition to identifying the soil constraints spatially, the limiting factor map serves as a decision-support tool for precision soil management. Despite acceptable subsoil conditions, interventions such as gypsum application or other agronomic interventions may be required in regions where topsoil sodicity (high ESP) is the primary restriction. Conversely, areas constrained by subsoil properties, such as low CEC, may be improved by the addition of organic matter or surface amendments. Through the integration of topsoil and subsurface data, the combined limiting factor map facilitates focused carbon-farming techniques, effective resource allocation, and site-specific remediation, thereby converting spatial diagnostics into useful management outcomes.

https://doi.org/10.5194/egusphere-2026-2466
Preprint. Discussion started: 20 May 2026

5. Conclusion:

Estimation of soil organic carbon is crucial for understanding soil productivity, as it guides farmers to take agronomic and soil management measures to enhance crop production. Generally, the BLA model facilitates quantifying the maximum amount of the target variable based on the predictor variable. While BLA has been predominantly used for crop yield, this study utilised this approach to predict the attainable SOC levels across the Australian grain growing regions and to identify the most limiting soil characteristics that limit SOC accumulation. This modelling technique is especially pertinent to the Australian setting, as these soils tend to have very low organic carbon and show significant regional geographic variability. This study showed that the mean value of Australian grain growing regions' topsoil SOC is 0.68 % (SD = 0.37), with an interquartile range of 0.45 to 0.82, which is regarded as very low for crop productivity and soil health as compared to Europe, for example. However, the BLA model found that, depending on the rainfall zone and related soil properties, attainable SOC levels can surpass 1% and even approach 2.5% under existing soil conditions. So, there is a potential gap between actual and attainable SOC, highlighting the substantial opportunities for carbon sequestration through better soil management techniques. Measuring this gap is essential for developing targeted interventions to improve SOC storage and foster climate-resilient, sustainable agriculture in Australia. This is crucial for a range of stakeholders and for providing benchmarks for land managers. The multivariate BLA model also enables the determination of soil constraints to SOC buildup with the spatial locations across the soil profile by generating a limiting factor map. The limiting factor map suggests that ameliorating the soil constraints that are manageable may increase the possibility for SOC sequestration. So, it facilitates farmers and land managers in executing site-specific soil management to improve soil health and crop productivity. Thus, the BLA model is a dynamic rather than a static system. If the existing adverse field conditions are removed, then the measured SOC will be different, and the boundary line will give a different value. Finally, this conceptual framework of BLA modelling can be reproducible, and can be customised with additional soil properties, such as total nitrogen and can be adapted to any grain growing farm throughout Australia. As more farms are added to the dataset, including grains and other industries, the scalable nature of the approach means the BLA can be applied to other farming systems and to different classification systems to the rainfall zones used here, for example Koppen climate classification.

Acknowledgments

We would like to acknowledge funding of this work by the Grains Research and Development Corporation (GRDC) through the ‘3D PAWC and constraint mapping’ project (UOS2206-009RTX), as well as the valued collaboration of growers, consultants, and corporate businesses.

Code and Data availability

The data used in this study are from a privately owned farm and are subject to confidentiality restrictions; therefore, they are not publicly available. Codes with example data will be available upon request.

https://doi.org/10.5194/egusphere-2026-2466
Preprint. Discussion started: 20 May 2026

Author contributions

TFAB, PF, and SBK: Conceptualisation. NH: Data curation. BH and NH: Formal analysis. TFAB and PF: Funding acquisition. BH and NH: Investigation. BH, PF, DAS, NH, SBK, and TFAB: Methodology. TFAB and PF: Project administration. TFAB and PF: Resources. BH, DAS, and NH: Software. TFAB and PF: Supervision. BH and NH: Validation. BH: Visualisation. BH: Writing - original draft. BH, PF, DAS, NH, SBK, and TFAB: Writing - review and editing.

Declaration of generative AI and AI-assisted technologies in the writing process

During the preparation of this manuscript, the authors utilised the ChatGPT tool to improve the readability, clarity, and language of the article. After using this tool, the authors meticulously reviewed and revised the content as needed and take full responsibility for the content of the publication.

Declaration of Competing Interest

The authors have declared no conflict of interest

References

Al-Shammari, D., Filippi, P., Poole, S., Han, S., & Bishop, T.F.A. (under revision). Can a density-based boundary line analysis be used to identify within-field yield gaps and key limiting factors to crop production?. Crop & Pasture Science.

Ayoubi, S., Karchegani, P. M., Mosaddeghi, M. R., and Honarjoo, N.: Soil aggregation and organic carbon as affected by topography and land use change in western Iran, Soil and Tillage Research, 121, 18-26, 2012.

Beare, M., McNeill, S., Curtin, D., Parfitt, R., Jones, H., Dodd, M., and Sharp, J.: Estimating the organic carbon stabilisation capacity and saturation deficit of soils: a New Zealand case study, Biogeochemistry, 120, 71-87, 2014.
Breiman, L.: Random forests, Machine learning, 45, 5-32, 2001.

Brock, P., Muir, S., and Simmons, A.: LCA as a tool for targeted GHG mitigation in Australian cropping systems, Proceedings of the 9th International Conference on Life Cycle Assessment in the Agri-Food Sector (LCA Food 2014), San Francisco, California, USA, 8-10 October 2014, 167-175, American Center for Life Cycle Assessment, 2014.

Brockett, B. F., Prescott, C. E., and Grayston, S. J.: Soil moisture is the major factor influencing microbial community structure and enzyme activities across seven biogeoclimatic zones in western Canada, Soil biology and biochemistry, 44, 9-20, 2012.

Bui, E., Henderson, B., and Viergever, K.: Using knowledge discovery with data mining from the Australian Soil Resource Information System database to inform soil carbon mapping in Australia, Global biogeochemical cycles, 23, 2009.

Bünemann, E. K., Bongiorno, G., Bai, Z., Creamer, R. E., De Deyn, G., De Goede, R., Fleskens, L., Geissen, V., Kuyper, T. W., and Mäder, P.: Soil quality–A critical review, Soil biology and biochemistry, 120, 105-125, 2018.

https://doi.org/10.5194/egusphere-2026-2466
Preprint. Discussion started: 20 May 2026

Casanova, D., Goudriaan, J., Bouma, J., and Epema, G.: Yield gap analysis in relation to soil properties in direct-seeded flooded rice, Geoderma, 91, 191-216, 1999.

Castaldi, F., Hueni, A., Chabrillat, S., Ward, K., Buttafuoco, G., Bomans, B., Vreys, K., Brell, M., and van Wesemael, B.: Evaluating the capability of the Sentinel 2 data for soil organic carbon prediction in croplands, ISPRS Journal of Photogrammetry and Remote Sensing, 147, 267-282, 2019.

Cavagnaro, T. R.: Soil moisture legacy effects: impacts on soil nutrients, plants and mycorrhizal responsiveness, Soil Biology and Biochemistry, 95, 173-179, 2016.

Chen, S., Arrouays, D., Angers, D. A., Chenu, C., Barré, P., Martin, M. P., Saby, N. P., and Walter, C.: National estimation of soil organic carbon storage potential for arable soils: A data-driven approach coupled with carbon-landscape zones, Science of the Total Environment, 666, 355-367, 2019.

Chenu, C., Angers, D. A., Barré, P., Derrien, D., Arrouays, D., and Balesdent, J.: Increasing organic stocks in agricultural soils: Knowledge gaps and potential innovations, Soil and Tillage Research, 188, 41-52, 2019.

Churchman, G. J., Singh, M., Schapel, A., Sarkar, B., and Bolan, N.: Clay minerals as the key to the sequestration of carbon in soils, Clays and Clay Minerals, 68, 135-143, 2020.

Clara, L., Fatma, R., Viridiana, A., and Liesl, W.: Soil organic carbon: the hidden potential, Rome: Food and Agriculture Organization of the United Nations, 2017.

Cleveland, W. S. and Devlin, S. J.: Locally weighted regression: an approach to regression analysis by local fitting, Journal of the American statistical association, 83, 596-610, 1988.

Drenovsky, R. E., Steenwerth, K. L., Jackson, L. E., and Scow, K. M.: Land use and climatic factors structure regional patterns in soil microbial communities, Global Ecology and Biogeography, 19, 27-39, 2010.

Drexler, S., Broll, G., Flessa, H., and Don, A.: Benchmarking soil organic carbon to support agricultural carbon management: A German case study#, Journal of Plant Nutrition and Soil Science, 185, 427-440, 2022.

Feng, W., Plante, A. F., and Six, J.: Improving estimates of maximal organic carbon stabilization by fine soil particles, Biogeochemistry, 112, 81-93, 2013.

Filippi, P., Whelan, B. M., and Bishop, T. F.: Proximal and remote sensing–what makes the best farm digital soil maps?, Soil Research, 62, 2024.

Filippi, P., Jones, E. J., Ginns, B. J., Whelan, B. M., Roth, G. W., and Bishop, T. F.: Mapping the depth-to-soil pH constraint, and the relationship with cotton and grain yield at the within-field scale, Agronomy, 9, 251, 2019.

Franzluebbers, K., Weaver, R., Juo, A., and Franzluebbers, A.: Carbon and nitrogen mineralization from cowpea plants part decomposing in moist and in repeatedly dried and wetted soil, Soil Biology and Biochemistry, 26, 1379-1387, 1994.

https://doi.org/10.5194/egusphere-2026-2466
Preprint. Discussion started: 20 May 2026

Friedman, J. H.: A variable span smoother, 1984.

Fujisaki, K., Chapuis-Lardy, L., Albrecht, A., Razafimbelo, T., Chotte, J.-L., and Chevallier, T.: Data synthesis of carbon distribution in particle size fractions of tropical soils: Implications for soil carbon storage potential in croplands, Geoderma, 313, 41-51, 2018.

Gallant, J., Wilson, N., Dowling, T., Read, A., and Inskeep, C.: SRTM-derived 1 second digital elevation models version 1.0, Geoscience Australia, 2011, https://pid.geoscience.gov.au/dataset/ga/122551

Georgiou, K., Jackson, R. B., Vindušková, O., Abramoff, R. Z., Ahlström, A., Feng, W., Harden, J. W., Pellegrini, A. F., Polley, H. W., and Soong, J. L.: Global stocks and capacity of mineral-associated soil organic carbon, Nature communications, 13, 3797, 2022.

Gregorich, E., Carter, M., Angers, D., and Drury, C.: Using a sequential density and particle-size fractionation to evaluate carbon and nitrogen storage in the profile of tilled and no-till soils in eastern Canada, Canadian journal of soil science, 89, 255-267, 2009.

Grains Research and Development Corporation (GRDC): Growing regions, available at: https://grdc.com.au/about/our-industry/growing-regions (last access: 16 April 2026), 2024.

Grundy, M. J., Viscarra Rossel, R. A., Searle, R. D., Wilson, P. L., Chen, C., and Gregory, L. J.: The soil and landscape grid of Australia, Soil Research, 53, 835–844, 2015, https://doi.org/10.1071/SR15191

Hajjarpoor, A., Soltani, A., Zeinali, E., Kashiri, H., Aynehband, A., and Vadez, V.: Using boundary line analysis to assess the on-farm crop yield gap of wheat, Field Crops Research, 225, 64-73, 10.1016/j.fcr.2018.06.003, 2018.

Hassink, J.: The capacity of soils to preserve organic C and N by their association with clay and silt particles, Plant and soil, 191, 77-87, 1997.

Hobley, E., Wilson, B., Wilkie, A., Gray, J., and Koen, T.: Drivers of soil organic carbon storage and vertical distribution in Eastern Australia, Plant and Soil, 390, 111-127, 2015.

Huang, X., Wang, L., Yang, L., and Kravchenko, A. N.: Management Effects on Relationships of Crop Yields with Topography Represented by Wetness Index and Precipitation, Agronomy Journal, 100, 1463-1471, 10.2134/agronj2007.0325, 2008.

Isbell, R. F.: The Australian soil classification, rev. edn., CSIRO Publishing, Melbourne, 2002.

Jenny, H.: Factors of soil formation: a system of quantitative pedology, Courier Corporation, 1994.

Jenny, H.: The soil resource: origin and behavior, Springer Science & Business Media, 2012.

https://doi.org/10.5194/egusphere-2026-2466
Preprint. Discussion started: 20 May 2026

Jien, S.-H., Minasny, B., Yang, B.-J., Liu, Y.-T., Yen, C.-C., Ocba, M. A., Zhang, Y.-T., and Syu, C.-H.: Enhancing Soil Carbon Storage: Developing high-resolution maps of topsoil organic carbon sequestration potential in Taiwan, Geoderma, 459, 117369, 2025.

Jonard, M., Nicolas, M., Coomes, D. A., Caignet, I., Saenger, A., and Ponette, Q.: Forest soils in France are sequestering substantial amounts of carbon, Science of the Total Environment, 574, 616-628, 2017.

Karunaratne, S., Asanopoulos, C., Jin, H., Baldock, J., Searle, R., Macdonald, B., and Macdonald, L. M.: Estimating the attainable soil organic carbon deficit in the soil fine fraction to inform feasible storage targets and de-risk carbon farming decisions, Soil Research, 62, 2024.

Keshavarzi, A., Tuffour, H. O., Bagherzadeh, A., Tattrah, L. P., Kumar, V., Gholizadeh, A., and Rodrigo-Comino, J.: Using fuzzy-AHP and parametric technique to assess soil fertility status in Northeast of Iran, Journal of Mountain Science, 17, 931-948, 2020.

Kiani-Harchegani, M. and Sadeghi, S. H.: Practicing land degradation neutrality (LDN) approach in the Shazand Watershed, Iran, Science of the Total Environment, 698, 134319, 2020.

Kitchen, N., Drummond, S., Lund, E., Sudduth, K., and Buchleiter, G.: Soil electrical conductivity and topography related to yield for three contrasting soil–crop systems, Agronomy journal, 95, 483-495, 2003.

Lark, R. and Milne, A.: Boundary line analysis of the effect of water-filled pore space on nitrous oxide emission from cores of arable soil, European Journal of Soil Science, 67, 148-159, 2016.

Lark, R. M., Gillingham, V., Langton, D., and Marchant, B. P.: Boundary line models for soil nutrient concentrations and wheat yield in national-scale datasets, European Journal of Soil Science, 71, 334-351, 2020.

Lewandowski, I. and Schmidt, U.: Nitrogen, energy and land use efficiencies of miscanthus, reed canary grass and triticale as determined by the boundary line approach, Agriculture, Ecosystems & Environment, 112, 335-346, 10.1016/j.agee.2005.08.003, 2006.

Ma, Y., Woolf, D., Fan, M., Qiao, L., Li, R., and Lehmann, J.: Global crop production increase by soil organic carbon, Nature Geoscience, 16, 1159-1165, 2023.

Makowski, D., Doré, T., and Monod, H.: A new method to analyse relationships between yield components with boundary lines, Agronomy for Sustainable Development, 27, 119-128, 10.1051/agro:2006029, 2007.

Malone, B., Searle, R., Stenson, M., McJannet, D., Zund, P., Román Dobarco, M., Wadoux, A. M. J.-C., Minasny, B., McBratney, A., and Grundy, M.: Update and expansion of the soil and landscape grid of Australia, Geoderma, 455, 117226, 2025, https://doi.org/10.1016/j.geoderma.2025.117226.

Meisner, A., De Deyn, G. B., de Boer, W., and van der Putten, W. H.: Soil biotic legacy effects of extreme weather events influence plant invasiveness, Proceedings of the National Academy of Sciences, 110, 9835-9838, 2013.

https://doi.org/10.5194/egusphere-2026-2466
Preprint. Discussion started: 20 May 2026

Milne, A., Ferguson, R., and Lark, R.: Estimating a boundary line model for a biological response by maximum likelihood, Annals of Applied Biology, 149, 223-234, 2006a.

Milne, A., Wheeler, H., and Lark, R.: On testing biological data for the presence of a boundary, Annals of Applied Biology, 149, 213-222, 2006b.

Minasny, B., Sulaeman, Y., and Mcbratney, A. B.: Is soil carbon disappearing? The dynamics of soil organic carbon in Java, Global Change Biology, 17, 1917-1924, 2011.

Minasny, B., McBratney, A. B., Malone, B. P., and Wheeler, I.: Digital mapping of soil carbon, Advances in agronomy, 118, 1-47, 2013.

Minty, B., Franklin, R., Milligan, P., Richardson, M., and Wilford, J.: The radiometric map of Australia, Exploration Geophysics, 40, 325-333, 2009.

Mirchooli, F., Kiani-Harchegani, M., Darvishan, A. K., Falahatkar, S., and Sadeghi, S. H.: Spatial distribution dependency of soil organic carbon content to important environmental variables, Ecological Indicators, 116, 106473, 2020.

Miti, C., Milne, A. E., Giller, K., Sadras, V., and Lark, R. M.: Exploration of data for analysis using boundary line methodology, Computers and Electronics in Agriculture, 219, 108794, 2024.

Nabiollahi, K., Golmohamadi, F., Taghizadeh-Mehrjardi, R., Kerry, R., and Davari, M.: Assessing the effects of slope gradient and land use change on soil quality degradation through digital mapping of soil quality indices and soil loss rate, Geoderma, 318, 16-28, 2018.

Ogorek, L. L. P., Gao, Y., Farrar, E., and Pandey, B. K.: Soil compaction sensing mechanisms and root responses, Trends in Plant Science, 30, 565-575, 2025.

Orgill, S. E., Condon, J. R., Conyers, M. K., Morris, S. G., Murphy, B. W., and Greene, R. S.: Parent material and climate affect soil organic carbon fractions under pastures in south-eastern Australia, Soil Research, 55, 799-808, 2017.

Patrignani, A., Lollato, R. P., Ochsner, T. E., Godsey, C. B., and Edwards, J. T.: Yield Gap and Production Gap of Rainfed Winter Wheat in the Southern Great Plains, Agronomy Journal, 106, 1329-1339, 10.2134/agronj14.0011, 2014.

Poeplau, C. and Don, A.: A simple soil organic carbon level metric beyond the organic carbon-to-clay ratio, Soil use and management, 39, 1057-1067, 2023.

Pozza, L. E., Filippi, P., Whelan, B., Wimalathunge, N. S., Jones, E. J., and Bishop, T. F. A.: Depth to sodicity constraint mapping of the Murray-Darling Basin, Australia, Geoderma, 428, 116181, 2022.

Preusser, S., Marhan, S., Poll, C., and Kandeler, E.: Microbial community response to changes in substrate availability and habitat conditions in a reciprocal subsoil transfer experiment, Soil Biology and Biochemistry, 105, 138-152, 2017.

https://doi.org/10.5194/egusphere-2026-2466
Preprint. Discussion started: 20 May 2026

Prout, J. M., Shepherd, K. D., McGrath, S. P., Kirk, G. J., Hassall, K. L., and Haefele, S. M.: Changes in organic carbon to clay ratios in different soils and land uses in England and Wales over time, Scientific Reports, 12, 5162, 2022.

Richter, D. d. and Yaalon, D. H.: "The changing model of soil" revisited, Soil Science Society of America Journal, 76, 766-778, 2012.

Roberts, D., Wilford, J., and Ghattas, O.: Exposed soil and mineral map of the Australian continent revealing the land at its barest, Nature Communications, 10, 5297, 2019.

Roberton, S. D., Bennett, J. M., Lobsey, C. R., & Bishop, T. F.: Assessing the sensitivity of site-specific lime and gypsum recommendations to soil sampling techniques and spatial density of data collection in Australian agriculture: a pedometric approach, Agronomy, 10(11), 1676, 2020.

Sanderman, J., Hengl, T., and Fiske, G. J.: Soil carbon debt of 12,000 years of human land use, Proceedings of the National Academy of Sciences, 114, 9575-9580, 2017.

Schmidt, U., Thöni, H., and Kaupenjohann, M.: Using a boundary line approach to analyze N2O flux data from agricultural soils, Nutrient Cycling in Agroecosystems, 57, 119-129, 2000.

Schnug, E., Heym, J., and Murphy, D. P.: Boundary line determination technique (BOLIDES).: In Site-Specific Management for Agricultural Systems, edited by: Robert, P. C., Rust, R. H., and Larson, W. E., 899–908, ASA-CSSA-SSSA, Madison, WI, 1995.

Schnug, E., Heym, J., and Achwan, F.: Establishing critical values for soil and plant analysis by means of the boundary line development system (BOLIDES), Communications in Soil Science and Plant Analysis, 27, 2739–2748, 1996.

Shatar, T. and McBratney, A.: Boundary-line analysis of field-scale yield response to soil properties, The Journal of Agricultural Science, 142, 553-560, 2004.

Soinne, H., Keskinen, R., Tähtikarhu, M., Kuva, J., and Hyväluoma, J.: Effects of organic carbon and clay contents on structure-related properties of arable soils with high clay content, European Journal of Soil Science, 74, e13424, 2023.

Tilse, M. J., Bishop, T. F., Triantafilis, J., and Filippi, P.: Mapping the impact of subsoil constraints on soil available water capacity and potential crop yield, Crop and Pasture Science, 73, 636-651, 2022.

Tipping, E., Davies, J., Henrys, P., Kirk, G. J., Lilly, A., Dragosits, U., Carnell, E. J., Dore, A., Sutton, M., and Tomlinson, S.: Long-term increases in soil carbon due to ecosystem fertilization by atmospheric nitrogen deposition demonstrated by regional-scale modelling and observations, Scientific Reports, 7, 1890, 2017.

Tittonell, P. and Giller, K. E.: When yield gaps are poverty traps: The paradigm of ecological intensification in African smallholder agriculture, Field Crops Research, 143, 76-90, 2013.

https://doi.org/10.5194/egusphere-2026-2466
Preprint. Discussion started: 20 May 2026

Tittonell, P., Shepherd, K. D., Vanlauwe, B., and Giller, K. E.: Unravelling the effects of soil and crop management on maize productivity in smallholder agricultural systems of western Kenya—An application of classification and regression tree analysis, Agriculture, ecosystems & environment, 123, 137-150, 2008.

Turicchi, J., O'Driscoll, R., Finlayson, G., Duarte, C., Palmeira, A. L., Larsen, S. C., Heitmann, B. L., and Stubbs, R. J.: Data imputation and body weight variability calculation using linear and nonlinear methods in data collected from digital smart scales: simulation and validation study, JMIR mHealth and uHealth, 8, e17977, 2020.

Viscarra Rossel, R., Webster, R., Zhang, M., Shen, Z., Dixon, K., Wang, Y. P., and Walden, L.: How much organic carbon could the soil store? The carbon sequestration potential of Australian soil, Global Change Biology, 30, e17053, 2024.

Viscarra Rossel, R. A., Webster, R., Bui, E. N., and Baldock, J. A.: Baseline map of organic carbon in Australian soil to support national carbon accounting and monitoring under climate change, Global Change Biology, 20, 2953-2970, 2014.

von Liebig, J. F.: The natural laws of husbandry, Walton & Maberly1863.

Wagner, S., Cattle, S., and Scholten, T.: Contributions of clay and organic matter to soil aggregation and structural stability, Journal of Plant Nutrition and Soil Science, 170, 173-180, 2007.

Wang, J., Filippi, P., Haan, S., Pozza, L., Whelan, B., and Bishop, T. F.: Gaussian process regression for three-dimensional soil mapping over multiple spatial supports, Geoderma, 446, 116899, 2024.

Wang, N., Jassogne, L., van Asten, P. J., Mukasa, D., Wanyama, I., Kagezi, G., and Giller, K. E.: Evaluating coffee yield gaps and important biotic, abiotic, and management factors limiting coffee production in Uganda, European Journal of Agronomy, 63, 1-11, 2015.

Wang, S., Fan, J., Zhong, H., Li, Y., Zhu, H., Qiao, Y., and Zhang, H.: A multi-factor weighted regression approach for estimating the spatial distribution of soil organic carbon in grasslands, Catena, 174, 248-258, 2019.

Webb, R.: Use of the boundary line in the analysis of biological data, Journal of Horticultural Science, 47, 309-319, 1972.

Wenzel, W. W., Duboc, O., Golestanifard, A., Holzinger, C., Mayr, K., Reiter, J., and Schiefer, A.: Soil and land use factors control organic carbon status and accumulation in agricultural soils of Lower Austria, Geoderma, 409, 115595, 2022.

Wiesmeier, M., Hübner, R., Spörlein, P., Geuß, U., Hangen, E., Reischl, A., Schilling, B., von Lützow, M., and Kögel-Knabner, I.: Carbon sequestration potential of soils in southeast Germany derived from stable soil organic carbon saturation, Global change biology, 20, 653-665, 2014.

Xu, X., Shi, Z., Li, D., Rey, A., Ruan, H., Craine, J. M., Liang, J., Zhou, J., and Luo, Y.: Soil properties control decomposition of soil organic carbon: Results from data-assimilation analysis, Geoderma, 262, 235-242, 2016.

Zeraatpisheh, M., Bakhshandeh, E., Hosseini, M., and Alavi, S. M.: Assessing the effects of deforestation and intensive agriculture on the soil quality through digital soil mapping, Geoderma, 363, 114139, 2020.

https://doi.org/10.5194/egusphere-2026-2466
Preprint. Discussion started: 20 May 2026

1055

Appendix Fig. **A1: Digital Soil map of subsoil (30-60 cm) of the case study farm used in the BLA model as predictors**

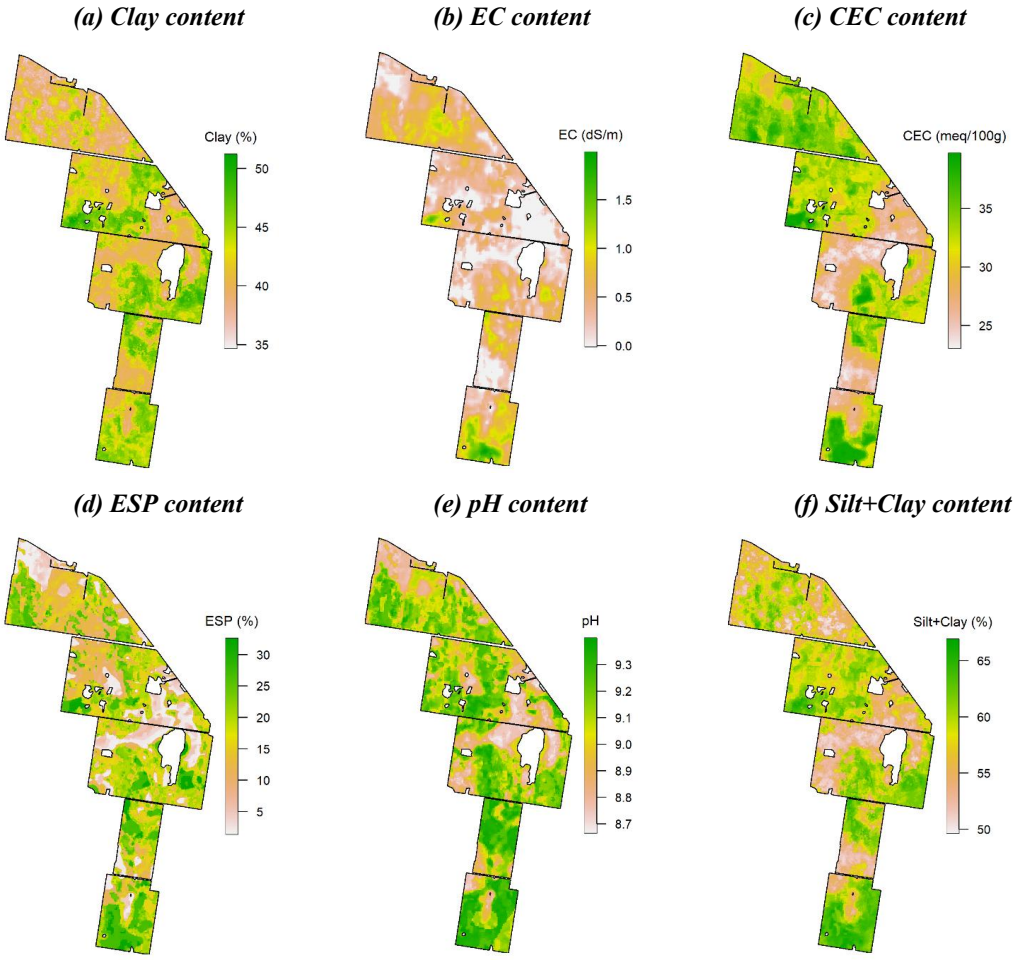

1060